國 立 交 通 大 學

電信工程研究所

碩 士 論 文
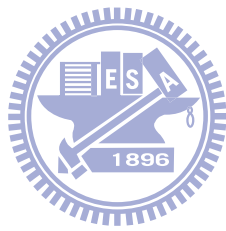
以幾何規劃方式求解矽鍺異質接面雙極性
電晶體摻雜輪廓最佳化之研究

Doping Profile Optimization of Silicon-Germanium
Heterojunction Bipolar Transistors via Geometric
Programming

研 究 生：陳英傑

指導教授：李義明 教授

中 華 民 國 九十九 年 八 月

以幾何規劃方式求解矽鍺異質接面

雙極性電晶體摻雜輪廓最佳化之研究

Doping Profile Optimization of Silicon-Germanium Heterojunction

Bipolar Transistors via Geometric Programming

研 究 生：陳英傑　　　　　　　　　　　Student：Ying-Chieh Chen

指導教授：李義明 博士　　　　　　　　Advisor：Dr. Yiming Li

國 立 交 通 大 學

電 信 工 程 研 究 所

碩 士 論 文

A Thesis

Submitted to Institute of Communications Engineering

College of Electrical Engineering and Computer Engineering

National Chiao Tung University

in partial Fulfillment of the Requirements
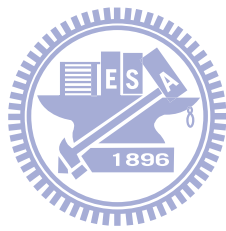
for the Degree of

Master

in

Electrical Engineering

Augest 2010

Hsinchu, Taiwan

中華民國九十九年八月

以幾何規劃方式求解矽鍺異質接面雙極性電晶體摻雜輪廓最佳化之研究

學生：陳英傑　　　　　　　　　　　　指導教授：李義明 博士

國立交通大學電信工程研究所碩士班

摘　　　　要

隨著高頻電路應用需求之提升，矽鍺(SiGe)異質介面雙極性電晶體(HBTs)的截止操作頻率(Cut-off frequency)也一直不斷的上升。而藉由調整基極的摻雜輪廓，可以增加矽鍺異質介面雙極性電晶體的操作速度。然而，設計基極的摻雜輪廓往往需要經由經驗法則反覆地嘗試而耗費許多時間與金錢成本。

幾何規劃(Geometric programming)為一種數學的最佳化問題，近年來常常被應用在科學與工程問題。藉由凸函數轉換與對偶定理，以及內點法演算方法(Interior point method)與電腦近幾十年來電腦計算能力的提升，我們可以迅速求解具大規模變數(Optimal variable)與限制式(Constraints)的幾何規劃問題，並且求得全域最佳解(Global solution)。

本論針對基極矽鍺摻雜輪廓設計寫成一幾何規劃問題。首先將矽鍺異質介面雙極性電晶體的截止頻率數學模型推導成與矽鍺摻雜輪廓有關的連續積分函數。接著，將此連續積分函數做離散(Discretization)，並將矽鍺摻雜輪廓表示為與基極位置(Base region)有關之離散的空間變數。透過以上的估計，我們可以把截止頻率表示成一特殊的函數—正多項式(*Posynomial*) ，而可將此非線性的最佳化問題轉成一幾何規劃問題，並以內點法求解。在不失工程準確性的要求下，此方法有效地提供了快速的矽鍺摻雜輪廓萃取。

為了驗證最佳化模型的準確度，我們以二維度(2-D)元件模擬器對異質介面雙極性電晶體模型中參數與元件特性做初步校估。結果顯示 23%濃度的梯型形鍺摻雜輪廓可以讓電流增益(Current gain)最大，其值約為 1100，比 0%濃度(傳統雙極性電晶體)的電流增益(約為 200)大；而 12.5%的鍺濃度與三角形的摻雜輪廓可以讓電晶體達到 254GHz 的截止操作頻率，也提升了傳統雙極性電晶體的截止操作頻率(約為 71GHz)。

　　總之，本研究已運用幾何規劃數學方法來求解矽鍺異質接面雙極性電晶體最佳摻雜輪廓。此研究有助於電腦模擬器的最佳化功能設計，對於半導體大廠之技術能力提升有正面之助益。

Abstract

As the the need of high frequency circuits, the speed of silicon-germanium (SiGe) heterojunction bipolar transistors (HBTs) has been dramatically increased. It is known that the speed of HBTs is dominated by the base transit time, which is influenced by the doping profile in the base region and the Ge concentration. However, to design the doping profile of HBTs requires lots of empirical experiences and time-consuming try-and-error rounds.

Geometric programming (GP) is a type of mathematical optimization problem, recently used in applied science and engineering widely. Based on the transformation of the geometric programming into convex form and the duality theory, also benefited from the interior point method and nowadays computing power, we can solve geometric programming problem with large scale optimal variables and constraints efficiently and globally.

In this study, the design of the doping profile and Ge-dose concentration for SiGe HBTs are mathematically formulated and solved by the technique of geometric programming. At

first, we derive the cut-off frequency model as an integral of Si doping profile and Ge-dose. Then, then discretization of the integral function according to the base region, is applied to obtain the discretized optimal variables of doping profile. Base upon the aforementioned approximation, we could derive the cut-off frequency model as a *posynomial* function; after that, the interior point method is employed to solve the well-formulated geometric programming. This methodology provides an efficient mechanism to extract the Si doping profile and Ge-dose.

The solution calculated by the GP method is guaranteed to be a global optimal. The accuracy of the adopted numerical optimization technique is first confirmed by comparing with a two-dimensional device simulation. The result of this study shows that a 23 % Ge fraction have the maximum current gain, about 1100, which higher than the 0 % Ge fraction (BJT), about 200. Furthermore, a 12.5% Ge may maximize the cut-off frequency for the explored device, where a 254 GHz cut-off frequency is achieved, high than the 0 % Ge fraction case, about 71 GHz.

In summary, we have successfully optimized the doping profile of SiGe HBTs using GP method. The results of this study may benefit the technology computer-aided design tool in semiconductor industry.

親從小到大仔細耐心對我的細心呵護，父親永遠不辭勞苦的在經濟上對我付出，已及懂事的妹妹在我讀研究所以來一直對我的支持，讓我能專注於課業研究中。在此謹將我的碩士論文，獻給所有關心，鼓勵及幫助過我的人。

陳英傑　謹誌

中華民國九十九年八月

于風城交大

平行與科學計算實驗室

Contents

List of Tables

List of Figures

Chapter 1

Introduction

This chapter first briefs the history of Silicon-germanium (SiGe) heterojunction bipolar transistors (HBTs) and the background of SiGe HBTs doping profile design. In the section 2, the history of optimization and the classification of optimization problems are discussed. Finally, we present the motivation and introduce the study of this thesis.

1.1   History and Background of SiGe HBTs

In this section, we brief the history of SiGe HBTs, and discuss the background of doping profile design of SiGe HBTs.

1.1.1   History of SiGe HBTs

SiGe technology is SiGe heterojunction bipolar transistors, has undergone substantial development for nearly two decades. SiGe HBT structure was first proposed in 1987 [1]. In 1990, a SiGe HBTs with 75 GHz cut-off frequency is investigated; in the same year, the circuit application using this SiGe HBT's device were demonstrated [2-3].

The first SiGe BiCMOS circuit was demonstrated in 1992 [4] and the first large-scale integrated circuit based on this topology was sequently reported in 1993 [5]; The 100 GHz frequency response SiGe HBTs were demonstrated in 1993-1994 [6-8], and the first SiGe HBT technology fabricated on 200-mm wafers were in 1994 [9]. During this ten years development, various SiGe HBT technologies had been demonstrated based on different SiGe epitaxial growth techniques [10-18], and in the 1994-1998, the practical digital and microwave high frequency applications had been proposed based on the SiGe epitaxial growth technologies [19-28], the detailed review paper about the aforementioned history of HBTs could be found in [29].

Recently, the SiGe HBTs have demonstrated cut-off frequency higher than 200 GHz [30-31], and the high frequency, great power performance and low noise amplifier application of SiGe HBTs was also developed [32-34].

1.1.2 Background of SiGe HBTs Doping Profile Design

The basis of SiGe technology is HBTs, which exhibits various merits over conventional Si bipolar junction transistors (BJTs) and silicon metal-oxide-semiconductor field effect transistors (MOSFETs) for implementation of high-frequency circuits [50-51]. Fig. 1.1(a) shows the circuit diagram of HBTs (BJTs), which is a three-terminal electronic device with doped semiconductor material and could be used in amplify or switching circuits. The structure of HBT (BJT) devices are shown in Fig. 1.1(b), composed by the emitter, base, and collector regions; The charge flow in a HBT (BJT) is due to bidirectional diffusion of charge carriers across a junction between two regions of different charge concentrations (emitter and base, or base and collector). The operation speed of HBTs are mainly dominated by the transit time of base region, which is strongly influenced by the doping profile and Ge concentration as shown in Fig. 1.1(c) in the base region (If the base is doped only one semiconductor material, the device is the so-called BJT) [35-52].

The determination of the doping profile and Ge concentration of the base region and thus is crucial for optimal design of SiGe HBTs in advanced high frequency communication circuits. Diverse engineering and theoretical approaches have been proposed to optimize the base transient time through optimization of the base doping profile [36-47]. An analytical optimum base doping profile by using variational calculus considering the dependence

of diffusion coefficient on base doping concentration was derived [37]. The analytical approach has been extended to consider the dependence of intrinsic carrier concentration on base doping concentration [38]. An iterative approach has also been proposed to obtain the optimum base doping profile [39], where the dependence of mobility and bandgap narrowing on the base doping concentration was considered [40].
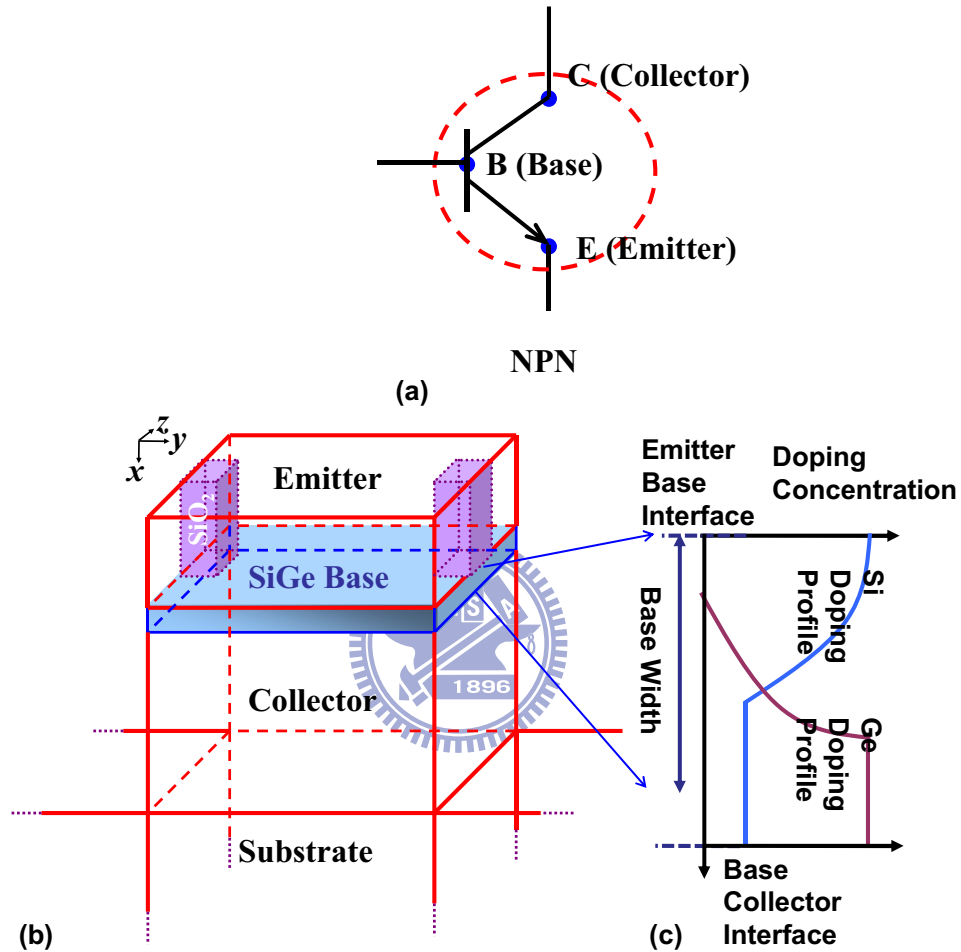
Figure 1.1: (a) The circuit diagram of HBTs (BJTs), which is a three-terminal electronic devices. (b) The illusion of HBTs (BJTs). The structure of HBT (BJT) devices are composed by the emitter, base, and collector regions; The charge flow in a BJT is due to bidirectional diffusion of charge carriers across a junction between two regions of different charge concentrations. (c) The designed Si and Ge doping profiles, which significantly influence the base transit time and sequentially raise the cut-off frequency and operate speed of HBT (BJT). If the base is doped only one semiconductor material, the device is the so-called BJT.

1.2   History and Background of Optimization

In this section, we list several important issues in the history of optimization theory and summary the classification of optimization problems.

1.2.1   History of Optimization

Optimization is the mathematical discipline to find the maxima and minima of functions, possibly subject to constraints. The first optimization algorithms are presented in 19th century. In 1826, J. B. J. Fourier formulated LP-problem for solving engineering problems, twenty years later; A. L. Cauchy presents the gradient method to search the solution in the minimum of functions. In 1947 G. Dantzig presented simplex method for solving LP-problems and in the same years, Von Neumann established the theory of duality for LP-problems. In 1951, Karush-Kuhn-Tucker theorem (KKT theorem) was proposed. The algorithms for unbounded optimization problems, such as quasi-Newton and conjugate gradient methods, were developed in 1954. In 1960s, the geometric programming had been known (Detailed introduction about geometric programming could be found in the chapter 2). In 1980s, the computers became more efficient, heuristic algorithms (such as genetic algorithm) for global optimization and large scale problems had greatly developed. In 1990s, the theory of interior point methods was established, and the algorithm to solve various optimization problems, based on the interior point theory had been developed till

nowadays [55, 57, 58].

1.2.2 Classification of Optimization Problems

A general classification of optimization problems for practical applications are shown in Fig. 1.2. The formulated optimization problems are first divided into two parts: model dependent and independent. The model independent problems could be solved using evolutionary algorithm, such as genetic algorithm [84]. The model dependent problems are general using search algorithm based on mathematical theory. According to the characteristic of the established model, the mathematical programming is classified as linear programming and nonlinear programming. If the nonlinear programming satisfied the convexity, we have the global solution, such as general convex programming and quadratic programming (least square problems) [58]. The geometric programming is one of the nonlinear program, however, we could transformed it as an convex programming (Detailed mathematical theory could be found in the section 2.3). Based on formulating (transforming) the practical problems as the aforementioned optimization problems, the well-developed software could solve them efficiently.
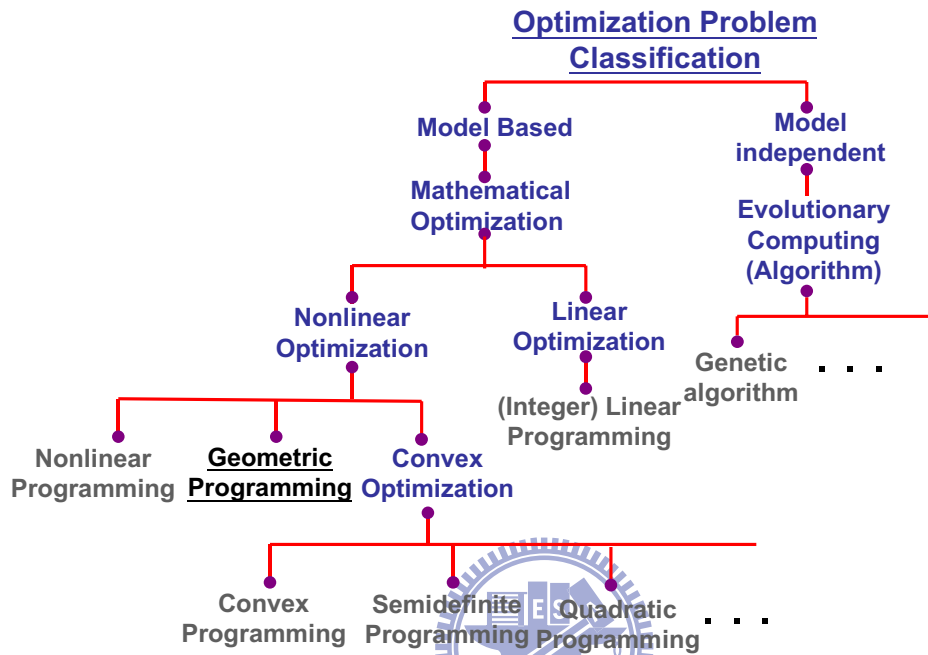
Figure 1.2: A general classification of optimization problems.The optimization problem could be mainly divided into two parts: model dependent (mathematical programming)/independent. The evolutionary algorithm could be employed to solve model independent problems, such as genetic algorithm. The model dependent problems are general using search algorithm based on mathematical theory. The mathematical programming is classified as linear programming and nonlinear programming. If the nonlinear programming satisfied the convexity, the global solution could be obtained, such as general convex programming and quadratic programming. The applied geometric programming in this thesis is one of the nonlinear programming which could be transformed into convex programming and solved efficiently.

1.3   Motivation of this Thesis

Due to the urgent demand of high-speed and large gain electron circuits, the GP approach is advanced to pursue the optimal Ge-dose as well as the doping profile as shown in Fig. 1.1(c) for the high cut-off frequency, or the high current gain in SiGe HBTs. In the previous work, the doping profile design for bipolar-junction transistor to optimize cut-off frequency and gain via GP had been proposed [36], however, the doping profile optimization for obtaining the electrical specifications for SiGe HBTs is laked. As a result, we provide a method to explore the SiGe HBTs doping profile optimization problem, and try to obtain higher cut-off frequency and current gain than the traditional BJT.

1.4 Objectives

In this thesis, the design of HBTs is first expressed as a special form of an optimization problem, the so-called GP, which can be transformed to a convex optimization problem, and then solved efficiently. The background doping profile is adjustable to improve the cut-off frequency and current gain. The result shows that a 23% Ge fraction may maximize the current gain, where a factor, current gain divided by the emitter Gummel number, of 1100 is attained. Furthermore, to maximize the cut-off frequency of HBTs, a Ge-dose concentration of 12.5% is used, where the cut-off frequency can achieve 254 GHz. Note that the accuracy of the developed optimization technique has been confirmed by comparing it with that of a two-dimensional (2D) device simulation [84-88]. This study successfully considers the device characteristics and manufacturing limitation as a GP model and the result may provide an insight into the design of SiGe HBTs.

1.5   Outline

The thesis is organized as follows. In chapter 2, we brief the history and background of GP. In chapter 3, GP formulation of the design of HBTs and manufacturing limitation are described. In chapter 4, the optimized cut-off frequency and current gain are discussed according to the calculated results. Finally, we draw conclusions and suggest future work.

Chapter 2

The Geometric Programming
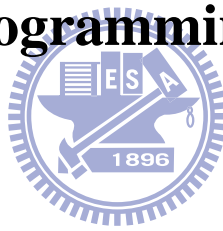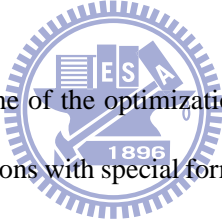
This chapter introduces the background of geometric programming. The content starts form giving the definition of the specifically types of functions of *monomial* and *posynomial* and geometric programming in standard form. Section 2 presents the convex problems converted from the geometric programming with many desirable properties and have a duality theory with them. The modern interior-point method is also briefed and the proceeding of solving the geometric programming is also discussed in this section. After that, some available tools to solve geometric programming as well as GP in convex form, and the sensitive/trade-off analysis are investigated. Finally, we list some practical applications of geometric programming.

2.1 Background and History

This section firstly introduces the background of geometric programming, and then its history and development is briefed.

2.1.1 Background of Geometric Programming

Geometric programming is one of the optimization approaches which is characterized by objective and constraint functions with special forms, *i.e.*, they are *posynomial* functions of the optimal variables. The name of geometric programming was from the original mathematical theory made extensive use of arithmetic-geometric mean inequality between sums and products of positive numbers. During the mathematical transformation, the geometric programming can be easily cast as convex programming (CP) problems. There are several advantages for the fact that GP can be reformulated as CP. For example, any starting point can find the global solution if the formulated optimization problem is feasible, on the other hand, if the problem is infeasible, a certificate proves infeasibility is found. For the real world problem, the most important characteristic of the GP may be the recently developed interior-point methods that solve the GP in convex form globally and efficiently.

2.1.2   History of Geometric Programming

The geometric programming has been known since 1961, when Clarence Zener found that many cost minimization problems in engineering had a special form [53]. At this same time, a duality theory for nonlinear programming, and a mathematical framework of geometric programming based upon its duality theory is proposed [54]. In 1967 to 1970, three books: Geometric Program [55], Engineering Designed by Geometric Programming [56] and Applied Geometric Programming [57] discussed the theoretical and practical aspects of geometric programming and established the fundamental groundwork of geometric programming. In recent years, GP has been applied to solve the electrical engineering problems (see Sec.2.4).

2.2   The Terminology of Geometric Programming

This section starts from the definition of different functions related to geometric programming and then introduces the geometric programming in standard form.

2.2.1 Monomial Functions

Let f denote n real positive variables, and $x = (x_1, \ldots, x_n)$ a vector composed by x_i. A real valued function f of x, with the form:

$$f(x) = cx_1^{a_1} x_2^{a_2} \ldots x_n^{a_n}, \tag{2.1}$$

where $c > 0$ and a_i are real numbers, is called a *monomial* function, or a *monomial*. Note that exponents can be any real numbers, including fractional or negative which is different with the standard definition from algebra in which the coefficients must be nonnegative integers. We refer to the constant c as the coefficient of the *monomial*, and we refer to the constants $a_1, \ldots, a_n$ as the exponents of the *monomial*. For example:

$$5.33x_1^{1.3} x_2^{-1.2}$$

is a *monomial* of the variables x_1 and x_2 with coefficient 5.33 and the exponents are 1.3 and -1.2 for x_1 and x_2. We list some composition rules for *monomial*:

1. any positive constant is a *monomial*, as is any variable;

2. *monomials* are closed under multiplication and division: if f and g are both *monomials*, then so are fg and f/g; (This includes scaling by any positive constant.) and

3. a *monomial* raised to any power is also a *monomial*.

2.2.2   Posynomial Functions

A sum of one or more *monomials*, *i.e.*, a function of the form:

$$g\left(X\right) = \sum_{k=1}^{k} c_k x_1^{a_{1k}} x_2^{a2k} ... x_n^{a_{nk}},$$ (2.2)

where $c_k > 0$, is called a *posynomial* function or, more a *posynomial* with k terms of the variables $x_1, ..., x_n$. The term '*posynomial*' is meant to suggest a combination of 'positive' and 'polynomial'. We list some composition rules for *monomial*:

1. any *monomial* is also a *posynomial*;

2. *posynomials* are closed under addition, multiplication, and positive scaling;

3. *posynomials* can be divided by monomials: If g is a *posynomial* and f is a *monomial*, then f/g is a *posynomial*; and

4. if γ is a nonnegative integer and f is a *posynomial*, then f^γ always makes sense and is a *posynomial*.

For example:

$$2x_1^{1.3}x_2^{-1.2} + 1.5x_3 + x_1 x_4^{5.5}$$

is a *posynomial* of the variables x_1 to x_4 with positive coefficient for every terms.

2.2.3   The Standard Form of Geometric Programming

A geometric program in standard form is an optimization problem of the form:

$$\text{Min} \quad f_0(x)$$

$$\text{s.t.} \quad f_i(x) \leq 1, i = 1, ..., m \ , \tag{2.3}$$

$$g_i(x) = 1, i = 1, ..., p$$

where f_i are *posynomial* functions, g_i are *monomials*, and x_i are the optimization variables.

(There is an implicit constraint that the variables must be positive, *i.e.*, $x_i > 0$.) We defined

the problem (2.3) as a geometric programming in standard form, to distinguish it from

extensions we will describe later. In a standard form of GP:

1. the objective must be *posynomial* (and it must be minimized); and

2. the equality constraints can only have the form of a *monomial* equal to one, and the

inequality constraints can only have the form of a *posynomial* less than or equal to one.

For example, consider the problem:

$$\text{Min} \quad x_1^{23}x_2^3 + x_1^6 x_3^{5.2}$$

$$\text{s.t.} \quad x_1^2 + x_2^5 x_3^1 \leq 1$$

$$x_2 + x_3 \leq 1 \quad ,$$

$$x_2 x_2^3 = 1$$

with variables x_1, x_2 and x_3. This is a GP in standard form, with $n = 3$ variables, $m = 2$

posynomial inequality constraints and $p = 1$ *monomial* equality constraints.

2.2.4   The Extension of Geometric programming

Several extensions are readily handled:

1. if f is a *posynomial* and g is a *monomial*, then the constraint $f(x) \leq g(x)$ can be handled

by expressing it as $f(x)/g(x) \leq 1$ (since f/g is *posynomial*). This includes as a special

case a constraint of the form $f(x) \leq b$, where f is *posynomial* and $b > 0$;

2. if g_1 and g_2 are both *monomial* functions, then we can handle the equality constraint

$g_1(x) = g_2(x)$ by expressing it as $g_1(x)/g_2(x) = 1$ (since g_1/g_2 is *monomial*); and

3. we can maximize a nonzero *monomial* objective function, by minimizing its reciprocal

(which is also a *monomial*).
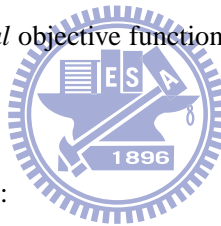
As an example, consider the problem:

$$\text{Min} \quad xz/y$$
$$s.t. \quad 2 \leq z \leq 5$$
$$x + y \leq z$$
$$xz = y^2$$

Using the simple transformations described above, we obtain the equivalent standard

form of GP:

$$\text{Min} \quad (xz)^{-1}y$$

$$s.t. \quad z/5 \le 1$$

$$2z^{-1} \le 1$$

$$xz^{-1} + yz^{-1} \le 1$$

$$xzy^{-2} = 1$$

2.3 Solving the Geometric Programming

This section shows how to solve the geometric programming. First we introduce the geometric programming in convex form, and the dual problem is discussed. Section 2.3.3 describes the interior-point methods to solve the prime and dual problem of geometric programming in convex form. Section 2.3.5 shows the softwares or tools to solve the geometric programming; finally, the trade-off and sensitivity analysis are introduced.

2.3.1 Geometric Programming in Convex Form

A geometric program can be reformulated as a convex optimization problem, *i.e.*, the problem of minimizing a convex function subject to convex inequality constraints and linear equality constraints. This is the key to our ability to globally and efficiently solve geometric programs. Using the variable transformation: $y_i = \log x_i$, and take the logarithm of

a *posynomial* f , we can further obtain:

$$h(y) = \log[f(e^{y_1}, ..., e^{y_n})] = \log(\sum_{k=1}^{t} e^{a_k^T y + b_k}), \qquad (2.4)$$

where $a_k^T = [a_1^k, ..., a_n^k]$ and $b_k = \log c_k$. It can be shown that h is a convex function of the new variable y: for all y, $z \in R^n$ and $1 \leq \lambda \leq 1$, we have:

$$h(\lambda y + (1 - \lambda)z) \leq \lambda h(y) + (1 - \lambda)h(z). \qquad (2.5)$$

Note that if the *posynomial* f is a *monomial*, then the transformed function is affine, *i.e.*, a linear function plus a constant. We can convert the standard geometric programming (2.3) in 2.2.3 into a convex programming by expressing it as:

$$\begin{aligned}
\text{Min} \quad & \log f_0(e^{y_1}, ..., e^{y_n}) = \log(\sum_{k=1}^{k_0} e^{a_{0k}^T y + b_{0k}}) \\
s.t. \quad & \log f_i(e^{y_1}, ..., e^{y_n}) = \log(\sum_{k=1}^{k_i} e^{a_{ik}^T y + b_{ik}}) \leq 0, i = 1, ..., m \\
& \log g_i(e^{y_1}, ..., e^{y_n}) = a_i^T y + b_i = 0, i = m + 1, ..., m + p
\end{aligned} \qquad (2.6)$$

This is the geometric programming in convex form. Convexity of the convex form geometric programming (2.6) has several important implications: we can use efficient interior-point methods to solve them, and there is a complete and useful duality, or sensitivity theory for them [58].

2.3.2 Dual Problem of Geometric Programming in Convex Form

The dual problem of GP in convex form (2.6) can be written as [54-55],

$$
\text{Max} \quad b_0^T v_0 - \sum_{j=1}^{k_0} v_{0,j} \log v_{0,j} + \sum_{i=1}^{m} \left(b_i^T v_i - \sum_{j=1}^{k_i} v_{i,j} \log(v_{i,j}/\lambda_i) \right) + \sum_{i=1}^{p} b_{m+i,1} u_i
$$

$$
s.t. \quad v_0 \geq 0, 1^T v_0 = 1
$$

$$
v_i \geq 0, 1^T v_i = \lambda_i, i = 1, ..., m \qquad\qquad , \quad (2.7)
$$

$$
\lambda_i \geq 0, i = 1, ..., m
$$

$$
\sum_{i=0}^{m} A_i^T v_i + \sum_{i=1}^{p} A_{m+i}^T u_i = 0
$$

where $v_i = (v_{i,1}, ..., v_{i,k_i})^T$, $c_{i,j}$ is the coefficient of the jth *monomial* term of the ith constraint and $A_i^T = [a_{i,1}, ..., a_{i,k_i}]$ is a matrix $\in R^{k_i \times n}$ whose column vectors $a_{i,j}$ are the exponents corresponding to the jth *monomial* term of the ith constraint. In this optimization problem, there are $\sum_{i=0}^{m} k_i + p$ optimal dual variables. The variables $v_{i,j}$ are associated with the jth inequality constraint. The variables μ_k are associated with the kth constraint. The dual problem of GP in convex form has some advantages from a computational point of view:

1. the concave object function whereas the object is maximized and the constraints are linear; and

2. the dual problem of this type has a significantly impact on the computational methods and theoretical developments for GP.

2.3.3   Interior-Point Methods

The foundation for modern interior-point methods, are based on the barrier methods. For solving the constrained nonlinear optimization problems, the penalty and barrier methods, which have a common motivation: finding an unconstrained minimizer of a composite function that reflects the original objective function as well as the presence of constraints. The interior-point methods are based on transforming constrained optimization to unconstrained optimization problem via logarithmic barrier function, is defined as:

$$B(x,\mu) \equiv f_0(x) - \mu \sum_{i=1}^{m+p} \ln f_i(x), \tag{2.8}$$

where μ is a positive scalar, called the barrier parameter. An important feature of $B(x,\mu)$ is that it retains the smoothness properties of $f_0(x)$ and $f_i(x)$ as long as $f_i(x) > 0$. If $\mu > 0$ and $\mu \rightarrow 0$, the characteristic of $B(x,\mu)$ is like $f_0(x)$. Intuition then suggests that minimizing $B(x,\mu)$ for a sequence of positive μ values converging to zero will cause the unconstrained minimizers of $B(x,\mu)$ to converge to a local constrained minimizer of the original problem [59-60].

2.3.4   The Procedure for Solving the Geometric Programming

In the solution procedure, we first formulate our problem as a geometric programming. Then we could transform the GP into convex form, and the corresponding dual problem could be formulated. After obtaining the prime and dual problem of GP in convex form,

we apply the logarithmic barrier function transformation to convert the constrained optimization problems into unconstrained ones. Finally, we could employ the general search algorithm such as gradient-method and Newton-method to solve this unconstrained optimization and the original solution could be inversely obtained. We give an algorithm as an example: given a strictly feasible point y, set $\mu^{(n=0)} > 0$, $\beta > 1$, and error tolerance $\varepsilon > 0$.

1. Centering step (gradient method for unconstrained optimization):

   Set $k = 0$ and error tolerance $\theta > 0$.

   1(a) Based on logarithmic barrier function (2.8), (2.6) could be transformed as:

   $$\text{Min } \phi(y) = \log(\sum_{k=1}^{k_0} e^{a_{0k}^T y + b_{0k}}) - \mu \sum_{i=1}^{m+p} \ln \left[\log(\sum_{k=1}^{k_i} e^{a_{ik}^T y + b_{ik}}) \right].$$

   1(b) Compute $\nabla \phi(y^{(k)})$, $\alpha_k = \arg \min \phi(y^{(k)} - \alpha \nabla \phi(y^{(k)}))$, $\alpha > 0$.

   1(c) Update: $y^{(k+1)} = y^{(k)} + \alpha_k \nabla \phi(y^{(k)})$.

   1(d) Stopping criterion: Quit if $\left| y^{(k+1)} - y^{(k)} \right| \leq \theta$.

   else

   1(e) Back to step 1(a).

2. Update: $y = y(\mu^{(n+1)})$.

3. Stopping criterion: Quit if $\left| y(\mu^{(n+1)}) - y(\mu^{(n)}) \right| \leq \varepsilon$.

else

4. Decrease $\mu^{(n+1)} = \frac{1}{\beta} \mu^{(n)}$.

5. Back to step 1.
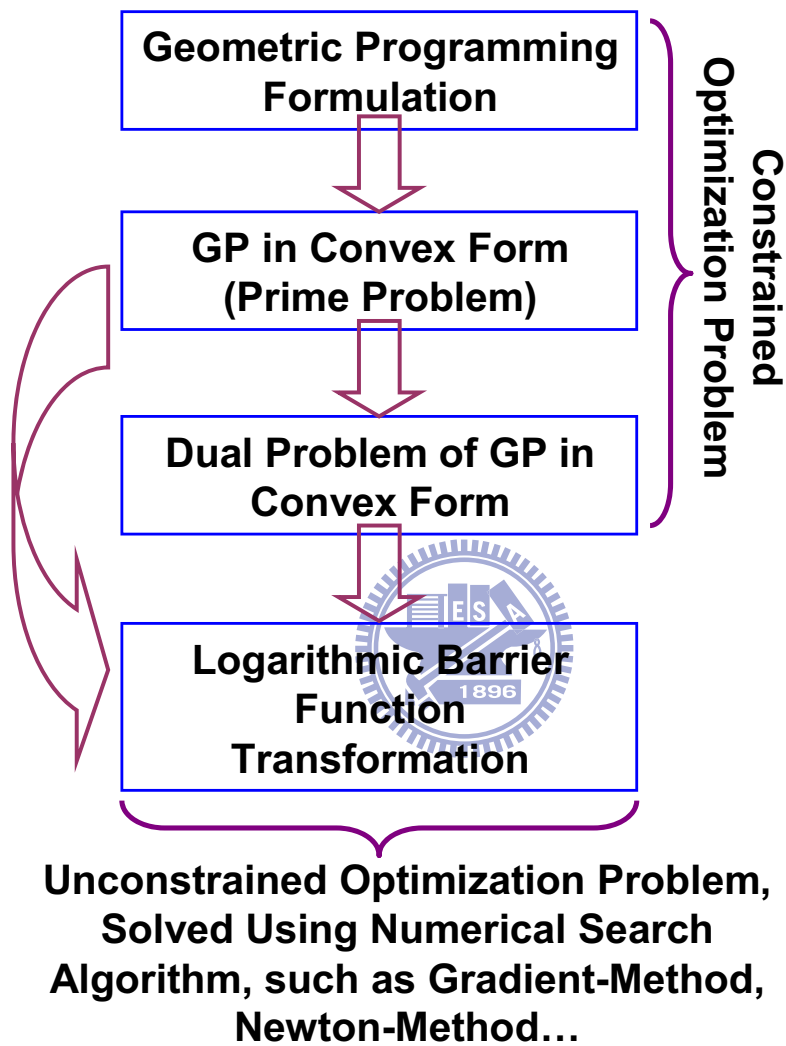
Figure 2.1: In the solution proceeding, we first formulate our problem
as geometric programming. Then we transform the GP in
convex form and also find its dual problems. After that, the
logarithmic barrier function transformation of the prime and
dual problem of GP in convex form is employed and this
unconstrained optimization problem could be solved
efficiently by general search algorithms.

2.3.5 Tools and Softwares for Geometric Programming

The nonlinear optimization solver using efficient interior-point algorithms [59] was developed since 1994, including geometric programming. Recently, the primal-dual interior-point methods are applied to solve the geometric programming [60]. The software: MINOS [61], LOQO [62] or LANCELOT [63], is also possible to solve the convex form problem with smooth objectives and constraints. These software could always obtain the global optimal solution based in the convex theory. In this work, we use the package ggplab [64] to solve our doping profile optimization problem in GP's form, and then we could obtain the solution efficiently and robustly.

2.3.6 Trade-Off Analysis

Suppose the right-hand sides of constraints are modified in the geometric programming (2.3) as follows:

$$
\begin{aligned}
\text{Min} \quad & f_0(x) \\
s.t. \quad & f_i(x) \leq u_i, i = 1, ..., m \\
& g_i(x) = v_i, i = 1, ..., p
\end{aligned} \quad \cdot \tag{2.9}
$$

If all of u_i and v_i are one, this modified geometric programming return to the original one. If $u_i \leq 1$, then the constraint $f_i(x) \leq u_i$ with a tighter restriction than the original i^{th} constraint; conversely if $u_i \geq 1$, it represents a *loosening* restriction of the constraint. For

example, the change in the specification $u_i = 0.9$ means that the ith constraint is tightened 10%, whereas $u_i = 1.1$ means that the ith constraint is loosened 10%. Supposed the $f_0^*(u, v)$ represent the optimal objective value of the modified geometric programming (2.9), as a function of the parameters $u = [u_1, u_2, ..., u_m]$ and $v = [v_1, v_2, ..., v_m]$, so the original objective value is $f_0^*(1, 1)$. In trade-off analysis, we observe the variation of objective function f_0^* as a function of small u and v. Then the change of objective function respect to the variation of constraint can be expressed as:

$$ S_i = \frac{\partial f_0^*/f_0^*}{\partial u_i/u_i}, \quad T_i = \frac{\partial f_0^*/f_0^*}{\partial v_i/v_i}. $$

These sensitivity numbers are dimensionless, since they express fractional changes per fractional change.

2.3.7   Sensitivity Analysis

Sensitivity analysis considers how small changes in the optimal variables affect the optimal objective value. Supposed the $f_0(x^*)$ represent the optimal objective value, we observe the variation of objective function f_0^* as a function of small perturbation of x^*, then the change of objective function respect to the variation of optimal variable can be expressed as:

$$ Z_i = \frac{\partial f_0^*/f_0^*}{\partial x_i/x_i}. $$

Optimal sensitivities can be very useful in practice. If a set of optimal variables are

solved, and has a small sensitivity, then small changes in the optimal variables won't affect the optimal value of the problem much. On the other hand, a solution set has a large sensitivity is one that (for small changes) will greatly change the optimal value, and the solution may be instable. Roughly speaking, an optimal value with a small sensitivity can be considered more strongly binding than one with a large sensitivity.

2.4   Practical Applications of Geometric Programming

There are wide varieties of application of geometric programming ranging from civil engineering to economics since 1960s:

1. **civil engineering**: optimal structural design [65], optimization of cofferdam problem [66];

2. **environmental engineering**: optimal wastewater treatment plants design [67], water quality management [68];

3. **chemical engineering**: Williamsotto process optimization [69], condenser designed [70];

4. **mechanical engineering**: space trusses design [71], optimal helical springs design [72];

5. **nuclear engineering**: nuclear systems design [73];

6. **economics**: marketing-mix problem [74], EOQ inventory model [75]; and

7. **electrical engineering**: CMOS op-amp design [76-78], gate sizing in digital circuits [79], LNA circuit parameters optimization [80-81] and temperature-aware floorplanning [82].

From the listed applications, we can know that GP has many contributions on many areas, although the GP is a very restrictive type of optimization problem. The detailed references about the aforementioned background of GP in the section 2 could refer [58, 76].

Chapter 3

Problem Formulation and Solution

Method

I n this chapter, we first formulate the optimal doping profile problem for SiGe HBTs, then the cut-off frequency model and GP formulation for the doping profile optimization is discussed. In Section 3, we show how to solve the formulated GP problem and list the corresponding implemented codes.

3.1 Problem Formulation

Figure 3.1 shows the studied SiGe HBTs device for the doping profile and Ge-dose concentration co-design, and also for a 2D device simulation. Mathematically, a doping profile

tuning problem for the high frequency property optimization of SiGe HBTs can be formulated as an optimization problem:

$$\text{Max} \quad f_t$$

$$s.t. \quad N_{min} \leq N_A(x) \leq N_{max},\ 0 \leq x \leq W_B$$

$$0 \leq G(x) \leq G_{\max},\ 0 \leq x \leq W_B$$

$$Ge_{AVG} = \frac{1}{W_B} \int_0^{W_B} G(x)dx \qquad\qquad , \qquad\qquad (3.1)$$

$$N_A(x) = bx^m, 0 \leq x \leq 0.05W_B$$

where f_t is the cut-off frequency; $N_A(x)$ and $G(x)$ are the base doping profiles for silicon and germanium, which are spatial-dependent positive functions over the interval $0 \leq x \leq W_B$ and x is depth from the interface of base and emitter into substrate. The base doping profile of silicon is lower than the doping level of emitter-base junction, $N_{\max}$, and higher than background doping, $N_{\min}$. The base doping profile of germanium is less than the maximum value G_{max}, and Ge_{AVG} is the average value of Ge fraction, which can be a given parameter ranging from 0 to 0.23 [36]. Assuming the manufacturing limitation, the maximum value of Ge fraction should be less or equal to the solubility of Ge atoms in silicon, such as 0.23 [36, 50-51]. In the present work, a peak base doping $N_{\max}$ of 1×10^{19} cm^{-3} at emitter edge of base and a minimum base doping $N_{\min}$ of 5×10^{16} cm^{-3} at collector edge of base have been chosen to include the heavy doping induced band gap

narrowing effect in the entire base region [36, 50-51]. W_B is the base width of the transistor, in which a neutral base width of 100 nm is chosen. And without loss of generality, we may assume the doping profile to be the form [36]:

$$N_A(x) = bx^m, 0 \le x \le 0.05W_B.$$

Here we assume $m = 0$ for a liner doping within 5% of the base width near the emitter-base junction.

3.1.1 Cut-off Frequency Model

For a SiGe HBT, the cut-off frequency f_t of a HBT is given by [50-51]:

$$\frac{1}{2\pi f_t} = \frac{C_{J,BE} + C_{J,BC}}{g_m} + R_C C_{J,BC} + \tau_F, \tag{3.2}$$

where $C_{J,BE}$ is the base–emitter junction or depletion layer capacitance, $C_{J,BC}$ is the base–collector junction or depletion layer capacitance, g_m is the transconductance, R_C is the collector resistance and τ_F is the forward transit time. The g_m and $C_{J,BE}$ in Eq. (3.2) could also be expressed as a function of doping profile:

$$g_m = \frac{q^2 A_{BE} n_{i0}^2}{KTG_B} \exp(\frac{qV_{BE}}{kT}), \tag{3.3}$$

and

$$C_{J,BE} = A_{BE} \left(\frac{q\varepsilon_{Si} N_A(0)}{2 (V_{bi} - V_{BE})} \right)^{0.5}, \tag{3.4}$$

where V_{BE} is the applied voltage across the emitter-base junction, V_{bi} is the built-in poten-

tial voltage, n_{i0} is the intrinsic carrier concentration in a undoped Si, ε_{Si} is the permittivity

of Si, A_{BE} is the area of the base-emitter junction, k is the Boltzmann constant, and T is

the temperature (Kelvin).
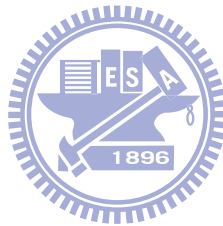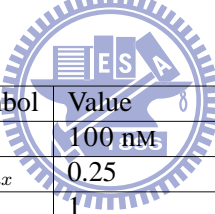
Table 3.1: The adopted parameters for the cut-off frequency model. The W_B is the base width, G_{max} is the maximin value of Ge-content, $C_{J,BC}$ is the base–collector junction capacitance, R_C is the collector resistance, q is the electrical charge, A_{BE} is the area of the base-emitter junction, k is the Boltzmann constant, T is the temperature (Kelvin), n_{i0} is the intrinsic carrier concentration in a undoped Si, $N_{\min}$ is the background doping concentration, $N_{\max}$ is the maximum doping concentration V_{BE} is the applied voltage across the emitter-base junction, V_{bi} is the built-in potential voltage, ε_{Si} is the permittivity of Si, and *b* is the constant.

Symbol	Value
W_B	100 нм
G_{max}	0.25
b	1
$C_{J,BC}$	0.8×10^{-12} F
R_C	0.4 kΩ
q	1.6×10^{-19}C
A_{BE}	0.25 μm^{-2}
k	8.617×10^{-5} eV / K
T	300° K
n_{i0}	1.4×10^{10} cm^{-3}
N_{min}	5×10^{16} cm^{-3}
N_{max}	1×10^{19} cm^{-3}
V_{BE}	1 V
V_{bi}	1.1 V
ε_{si}	1.04×10^{-12} F / cm^2

3.1.2   Forward Transit Time Model

The forward transit time in Eq. (3.2) are approximately composed by three components:

$$\tau_F = \tau_B + \tau_E + \tau_{BC}, \tag{3.5}$$

where τ_E is the emitter delay time and τ_{BC} is the base–collector depletion region transit time. The τ_{BC} could be expressed as:

$$\tau_{BC} = \frac{W_{BC}}{2v_{sat}}, \tag{3.6}$$

where the base–collector depletion width W_{BC} is determined by the collector doping concentration near the base–collector junction which we assume to be lower than the base doping concentration, and v_{sat} is the saturation velocity of electrons. The τ_E could be expressed as:

$$\tau_E = \left(\frac{W_E P_{Eq,E}}{2n_{i0}^2}\right)\left(\frac{\gamma^{-1}}{1 + k_{SiGe}Ge_{AVG}}\right)G_B, \tag{3.7}$$

where W_E is the width of the emitter region, $P_{Eq,E}$ is the equilibrium concentration of holes in the emitter, γ is the ratio of the effective density of states in SiGe to the effective density of states in silicon and k_{SiGe} are constants [36]. The G_B is the base Gummel number, which is also a function of $N_A(x)$ [50-51]:

$$G_B = \int_0^{W_B} \frac{N_A(x)n_{i0}^2}{D_n(x)n_i^2(x)}dx, \tag{3.8}$$

where $n_i(x)$ is the intrinsic carrier concentration in Si and $D_n(y)$ is the carrier diffusion

coefficient of Si, and both could be express as the function of doping profile:

$$n_i(x)^2 = n_{i0}^2 (\frac{N_A(x)}{Nref})^{\gamma_2}, \tag{3.9}$$

and

$$D_n(x) = D_{n0} \left(\frac{N_A(x)}{Nref} \right)^{-\gamma_1}, \tag{3.10}$$

where *Nref*, D_{n0} and γ_2 are constants [36]. Substituting Eqs. (3.9) and (3.10) into Eq. (3.8),

we have:

$$G_B = \frac{1}{Nref^{\gamma_1 - \gamma_2} D_{n0}} \int_0^{W_B} N_A(x)^{1+\gamma_1 - \gamma_2} dx. \tag{3.11}$$

3.1.3 Base Transit Time Model

The base transit time model in the optimization problem is given by [50-51], as shown

in below:

$$\tau_B = \int_0^{W_B} \frac{n_{i,SiGe}^2(x)}{N_A(x)} (\int_x^{W_B} \frac{N_A(y)}{n_{i,SiGe}^2(y) D_{n,SiGe}(y)} dy) dx, \tag{3.12}$$

where $n_{i,SiGe}(x)$ is the intrinsic carrier concentration in SiGe and $D_{n,SiGe}(y)$ is the carrier

diffusion coefficient of SiGe. The x- and y- directions in Eq. (3.12) are indicated in Fig.

3.1. The $n_{i,SiGe}(x)$ and $D_{n,SiGe}(y)$ depend on the profile of Si and Ge-dose [36, 50-51]:

$$n_{i,SiGe}^2(x) = \gamma n_{i,0}^2 \exp\left(\mu G(x)\right), \tag{3.13}$$

and

$$D_{n,SiGe}(y) = (1 + k_{SiGe}Ge_{AVG})D_{n0}\left(\frac{N_A(x)}{Nref}\right)^{\gamma_2}, \qquad (3.14)$$

substituting Eqs. (3.13) and (3.14) to Eq. (3.12), we have:

$$\tau_B = \frac{1}{Nref^{\gamma_1}D_{n0}(1 + k_{SiGe}Ge_{AVG})}\int\limits_0^{W_B}\exp(\mu G(x))N_A(x)^{\gamma_2-1}(\int\limits_x^{W_B}\frac{N_A(y)^{1+\gamma_1-\gamma_2}}{\exp(\mu G(y))}dy)dx.$$
$$(3.15)$$

3.1.4   Cut-off Frequency Model as A Function of Doping Profile

Substitute G_B of Eq. (3.11) into Eqs. (3.7) and (3.3), τ_{BC} of Eq. (3.6) and τ_E of Eq. (3.7) into τ_F of Eq. (3.5), and τ_B of Eq. (3.15), as well as Eqs. (3.3) to (3.5) into cut-off frequency model of Eq. (3.2), we have:

$$\frac{1}{2\pi f_t} = \frac{1}{Nref^{\gamma_1}D_{n0}(1+k_{SiGe}Ge_{AVG})}\int\limits_0^{W_B}\exp(\mu G(x))N_A(x)^{\gamma_2-1}(\int\limits_x^{W_B}\frac{N_A(y)^{1+\gamma_1-\gamma_2}}{\exp(\mu G(y))}dy)dx$$

$$+(\frac{W_E P E_{q,E}}{2n_{i0}^2})(\frac{\gamma^{-1}}{1+k_{SiGe}Ge_{AVG}})(\frac{1}{Nref^{\gamma_1-\gamma_2}D_{n0}}\int\limits_0^{W_B}N_A(x)^{1+\gamma_1-\gamma_2}dx) + \left(\frac{kT\varepsilon_{SiGe}}{n_{i0}^2 2q^3(V_{bi}-V_{BE})}\right)^{1/2}$$

$$\exp(-\frac{qV_{BE}}{kT}) \times N_A(0)^{1/2}(\frac{1}{Nref^{\gamma_1-\gamma_2}D_{n0}}\int\limits_0^{W_B}N_A(x)^{1+\gamma_1-\gamma_2}dx)(\frac{\gamma^{-1}}{1+k_{SiGe}Ge_{AVG}})$$

$$+\frac{C_{J,BC}kT}{q^{0.5}A_{BE}n_{i0}^2}\exp(-\frac{qV_{BE}}{kT})(\frac{\gamma^{-1}}{1+k_{SiGe}Ge_{AVG}})(\frac{1}{Nref^{\gamma_1-\gamma_2}D_{n0}}\int\limits_0^{W_B}N_A(x)^{1+\gamma_1-\gamma_2}dx) + \frac{W_{BC}}{2v_{sat}} + R_C C_{J,BC}$$
$$(3.16)$$

which strongly depends on doping profile of Si and Ge-dose.

3.1.5   SiGe HBTs Doping Profile Nonlinear Optimization

After substituting the cut-off frequency model of Eq. (3.16) into the original HBTs

doping profile designed problem of Eq. (3.1), we will have:

$$
\text{Max} \left(
\begin{aligned}
& \frac{2\pi}{Nref^{\gamma_1}D_{n0}(1+k_{SiGe}Ge_{AVG})} \int\limits_{0}^{W_B} \exp(\mu G(x))N_A(x)^{\gamma_2-1} \big(\int\limits_{x}^{W_B} \frac{N_A(y)^{1+\gamma_1-\gamma_2}}{\exp(\mu G(y))} dy \big) dx \\
& + 2\pi \big(\frac{W_E P E_{q,E}}{2n_{i0}^2} \big) \big(\frac{\gamma^{-1}}{1+k_{SiGe}Ge_{AVG}} \big) \big(\frac{1}{Nref^{\gamma_1-\gamma_2}D_{n0}} \int\limits_{0}^{W_B} N_A(x)^{1+\gamma_1-\gamma_2} dx \big) \\
& + 2\pi \left(\frac{kT\varepsilon_{SiGe}}{n_{i0}^2 2q^3(V_{bi}-V_{BE})} \right)^{1/2} \exp(-\frac{qV_{BE}}{kT})N_A(0)^{1/2} \big(\frac{1}{Nref^{\gamma_1-\gamma_2}D_{n0}} \int\limits_{0}^{W_B} N_A(x)^{1+\gamma_1-\gamma_2} dx \big) \\
& \big(\frac{\gamma^{-1}}{1+k_{SiGe}Ge_{AVG}} \big) + \frac{2\pi C_{J,BC}kT}{q^2 A_{BE}n_{i0}^2} \exp(\frac{qV_{BE}}{kT}) \big(\frac{\gamma^{-1}}{1+k_{SiGe}Ge_{AVG}} \big) \\
& \big(\frac{1}{Nref^{\gamma_1-\gamma_2}D_{n0}} \int\limits_{0}^{W_B} N_A(x)^{1+\gamma_1-\gamma_2} dx \big) + \frac{\pi W_{BC}}{v_{sat}} + R_C C_{J,BC}
\end{aligned}
\right)^{-1} ,
$$

$$
\begin{aligned}
s.t. \quad & N_{min} \leq N_A(x) \leq N_{max}, \ 0 \leq x \leq W_B \\
& 0 \leq G(x) \leq G_{\max}, \ 0 \leq x \leq W_B \\
& Ge_{AVG} = \frac{1}{W_B} \int\limits_{0}^{W_B} G(x)dx \\
& N_A(x) = bx^m, \ 0 \leq x \leq 0.05W_B
\end{aligned}
$$

(3.17)

where the objective function is composed by a two-dimension integral, and the Ge-dose is

in the exponential term, which is a nonlinear continues function and is hard to solve us-

ing the general optimization solver. For example, if we apply an evolutionary algorithm,

the doping profile function is hard to encode to solve; if using the nonlinear optimization

solution method, the corresponding KKT condition probably is difficult to calculate. As a

result, the technique of geometric programming transformation is employed in the follow-

ing sections.
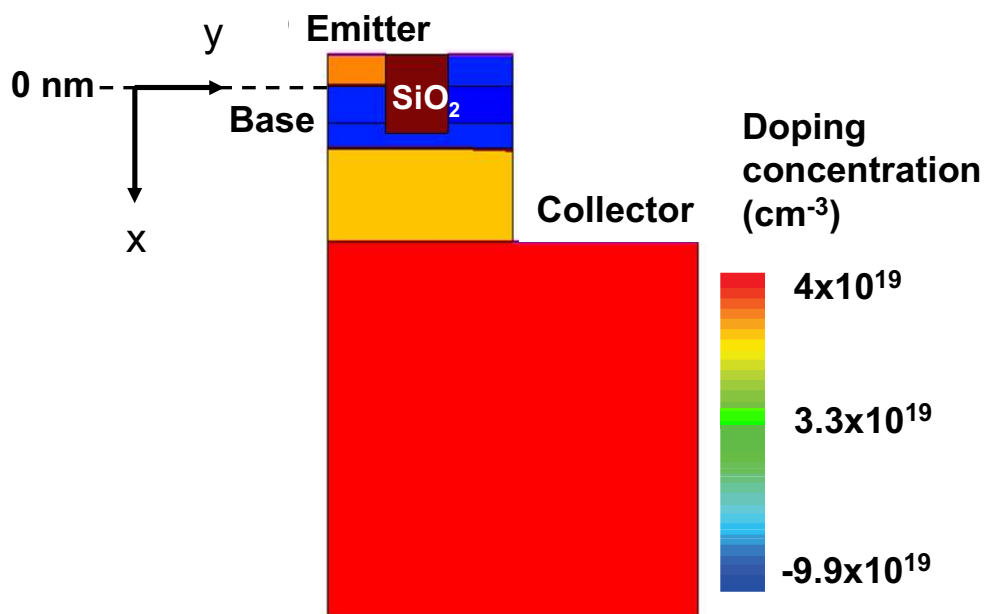
Figure 3.1: Illustration of the two-dimensional device structure of the explored SiGe HBT. The doping profile and Ge-dose concentration co-design, and also for a 2D device simulation are implemented in this specific structure.

3.2   GP Formulation for SiGe HBTs Doping Profile Optimization

In this section, we show how to formulate the general nonlinear SiGe HBTs doping profile optimization problem (3.17) into GP's form.

3.2.1   Taking Reciprocal for the Objective Function

For GP transformation, the nonlinear optimization problem (3.17) is formulated as:

$$
\text{Min} \quad \frac{1}{Nref^{\gamma_1} D_{n0}(1+k_{SiGe}Ge_{AVG})} \int_0^{W_B} \exp(\mu G(x)) N_A(x)^{\gamma_2-1} \left(\int_x^{W_B} \frac{N_A(y)^{1+\gamma_1-\gamma_2}}{\exp(\mu G(y))} dy \right) dx
$$

$$
+2\pi\left(\frac{W_E PE_{q,E}}{2n_{i0}^2}\right)\left(\frac{\gamma^{-1}}{1+k_{SiGe}Ge_{AVG}}\right)\left(\frac{1}{Nref^{\gamma_1-\gamma_2} D_{n0}} \int_0^{W_B} N_A(x)^{1+\gamma_1-\gamma_2} dx\right) + \left(\frac{kT\varepsilon_{SiGe}}{n_{i0}^2 2q^3(V_{bi}-V_{BE})}\right)^{1/2}
$$

$$
\exp\left(-\frac{qV_{BE}}{kT}\right) N_A(0)^{1/2} \left(\frac{1}{Nref^{\gamma_1-\gamma_2} D_{n0}} \int_0^{W_B} N_A(x)^{1+\gamma_1-\gamma_2} dx\right)\left(\frac{\gamma^{-1}}{1+k_{SiGe}Ge_{AVG}}\right)
$$

$$
+\frac{C_{J,BC}kT}{q^2 A_{BE}n_{i0}^2} \exp\left(-\frac{qV_{BE}}{kT}\right)\left(\frac{\gamma^{-1}}{1+k_{SiGe}Ge_{AVG}}\right)\left(\frac{1}{Nref^{\gamma_1-\gamma_2} D_{n0}} \int_0^{W_B} N_A(x)^{1+\gamma_1-\gamma_2} dx\right) + \frac{W_{BC}}{2v_{sat}}
$$

$$
+R_C C_{J,BC}
$$

$$
s.t. \quad N_{min} \le N_A(x) \le N_{max},\ 0 \le x \le W_B
$$

$$
0 \le G(x) \le G_{\max},\ 0 \le x \le W_B
$$

$$
Ge_{AVG} = \frac{1}{W_B} \int_0^{W_B} G(x)dx
$$

$$
N_A(x) = bx^m,\ 0 \le x \le 0.05W_B
$$

$$
(3.18)
$$

The effectiveness of maximizing the f_t is equal to minimizing the reciprocal of f_t.

3.2.2 Discretizing the Continuous Doping Profile Function

In the base transit time model (3.15) of SiGe HBT, the doping profile is continuous. To represent the doping profile as the discretized variables to be solved, the base region in Eq. (3.15) is first discretized to M regions, $x_i = iW_B/M, i = 0, 1, ..., M - 1$, and the continuous doping profile functions $N_A(x)$ and $G(x)$ can be transformed to $N_A(x_i)$ and $G(x_i), i = 0, 1, ..., M - 1$, as shown in Fig. 3.2;

$$\tau_B = \frac{W_B^2}{M^2 N ref^{\gamma_1} D_{n0}(1 + k_{SiGe}Ge_{AVG})} \sum_{i=0}^{M-1} \exp(uG(x_i)) N_A(x_i)^{\gamma_2 - 1} \sum_{j=i}^{M-1} \frac{N_A(x_j)^{1 + \gamma_1 - \gamma_2}}{\exp(uG(x_j))}.$$

(3.19)

Problem (3.19) is not a valid *posynomial* since it contains the optimal variables $G(x_i)$ in the exponential term. Fortunately, we can use the variable transformation as shown in Fig. 3.2:

$$L(x_i) = \exp(G(x_i)), i = 0, 1, ..., M - 1,$$

(3.20)

then Eq. (3.19) could be reexpressed as:

$$\tau_B = \frac{W_B^2}{M^2 N ref^{\gamma_1} D_{n0}(1 + k_{SiGe}Ge_{AVG})} \sum_{i=0}^{M-1} L(x_i)^u N_A(x_i)^{\gamma_2 - 1} \sum_{j=i}^{M-1} L(x_j)^{-u} N_A(x_j)^{1 + \gamma_1 - \gamma_2},$$

(3.21)

and the constraint of Ge-dose of Eq. (3.18) ($0 \leq G(x_i) \leq G_{\max}, i = 0, 1, ..., M - 1$) and

$(Ge_{AVG} = \frac{1}{M} \sum\limits_{i=0}^{M-1} G(x_i))$ is discretized and reformulated as:

$$1 \leq L(x_i) \leq \exp(G_{\max}), i = 0, 1, ..., M-1, \tag{3.22}$$

and

$$\begin{aligned} \exp(MGe_{AVG}) &= \exp\left[\sum_{i=0}^{M-1} G(x_i)\right] \\ &= \prod_{i=0}^{M-1} \exp G(x_i) = \prod_{i=0}^{M-1} L(x_i) \end{aligned} \tag{3.23}$$

respectively.

3.2.3 Derive the Summation Function of Doping Profile as Posynomial

For the summation of optimal variables of doping profiles Eq. (3.21) and G_B of Eq. (3.11), we define:

$$\begin{aligned} S_i &= \sum_{j=i}^{M-1} L(x_j)^{-u} N_A(x_j)^{1+\gamma_1-\gamma_2}, i = 0, 1, ..., M-1 \\ W_i &= \sum_{j=i}^{M-1} L(x_j)^{u} N_A(x_j)^{\gamma_2-1} S_j, i = 0, 1, ..., M-1 \quad, \\ b_i &= \sum_{j=i}^{M-1} N_A(x_j)^{1+\gamma_1-\gamma_2}, i = 0, 1, ..., M-1 \end{aligned} \tag{3.24}$$

and the above equations can also be expressed as backward recursions:

$$
\begin{aligned}
&S_{i+1} + L(x_i)^{-u} N_A(x_i)^{1+\gamma_1-\gamma_2} \le S_i, i = 0, 1, ..., M-2 \\[6pt]
&W_{i+1} + L(x_i)^{u} N_A(x_i)^{\gamma_2-1} S_i \le W_i, i = 0, 1, ..., M-2 \\[6pt]
&b_{i+1} + N_A(x_i)^{1+\gamma_1-\gamma_2} \le b_i, i = 0, 1, ..., M-2 \\[6pt]
&W_{M-1}^{-u} N_A(x_{M-1})^{1+\gamma_1-\gamma_2} = S_{M-1} \\[6pt]
&W_{M-1}^{u} N_A(x_{M-1})^{\gamma_2-1} S_{M-1} = W_{M-1} \\[6pt]
&N_A(x_{M-1})^{1+\gamma_1-\gamma_2} = b_{M-1}
\end{aligned}
\qquad . \qquad (3.25)
$$

During the above representation for the summation functions, we have the recursive *posynomial* inequality constraints (for every constraints, the left-hand sides of the inequalities are *posynomial*, and right-hand sides are *monomial*).

3.2.4 SiGe HBTs Doping Profile Optimization in GP's Form

In problem (3.18), we express the summation of Eqs. (3.21) by (3.24) and (3.25), replace the Ge-dose constraints by Eqs. (3.22) and (3.23) and then we have:

Min $\quad AW_0 + B_1 N_A(x_0)^{0.5} b_0 (1 + K_{SiGe} Ge_{AVG})^{-1} + B_2 b_0 (1 + K_{SiGe} Ge_{AVG})^{-1} + C$

s.t. $\quad N_{min} \leq N_A(x_i) \leq N_{max}, i = 0, 1, ..., M-1$

$\quad S_{i+1} + L(x_i)^{-u} N_A(x_i)^{1+\gamma_1-\gamma_2} \leq S_i, i = 0, 1, ..., M-2$

$\quad W_{i+1} + L(x_i)^u N_A(x_i)^{\gamma_2-1} S_i \leq W_i, i = 0, 1, ..., M-2$

$\quad b_{i+1} + N_A(x_i)^{1+\gamma_1-\gamma_2} \leq b_i, i = 0, 1, ..., M-2$

$\quad W_{M-1}^{-u} N_A(x_{M-1})^{1+\gamma_1-\gamma_2} = S_{M-1}$

$\quad W_{M-1}^u N_A(x_{M-1})^{\gamma_2-1} S_{M-1} = W_{M-1}$

$\quad N_A(x_{M-1})^{1+\gamma_1-\gamma_2} = b_{M-1}$

$\quad 1 \leq L(x_i) \leq \exp(G_{\max}), \ i = 0, 1, ..., M-1$

$\quad N_A(x_i) = b x_i^m, i = 0, 1, ..., 0.05M$

$\quad \exp(M Ge_{AVG}) = \prod_{i=0}^{M-1} L(x_i)$

$$\tag{3.26}$$

where *A*, *B* and *C* are collected doping profile independent constants. Note that $N_A(x_i)$ is the discretized variables of doping profile in base region; i, ranging between zero and M-1, is the uniformly spaced mesh points in the base region. Through these sets of variables,

$N_A(x_i)$, $L(x_i)$, S_i, W_i and b_i we can co-optimize the doping profile of Si and Ge in the

base region for different given Ge_{AVG} ranged from 0 to 0.23. Problem (3.26) is a GP since

the coefficients of objective function *A*, *B* and *C* are positive, and thus it is a *posynomial*

function; the left-hand sides of the inequalities are *posynomials* and the respect right-hand

sides are *monomial* functions; and the equality is a *monomial* equality. For justifying the

solution of the formulated GP of Eq. (3.26), we apply the variable transformation as section

2.3.1:

$$
\begin{aligned}
&N_A(x_i) = \exp(\alpha_i), i = 0, 1, ..., M-1 \\
&L(x_i) = \exp(\beta_i), i = 0, 1, ..., M-1 \\
&S_i = \exp(\eta_i), i = 0, 1, ..., M-1 \\
&W_i = \exp(\pi_i), i = 0, 1, ..., M-1 \\
&b_i = \exp(\lambda_i), i = 0, 1, ..., M-1
\end{aligned}
\qquad , \qquad (3.27)
$$
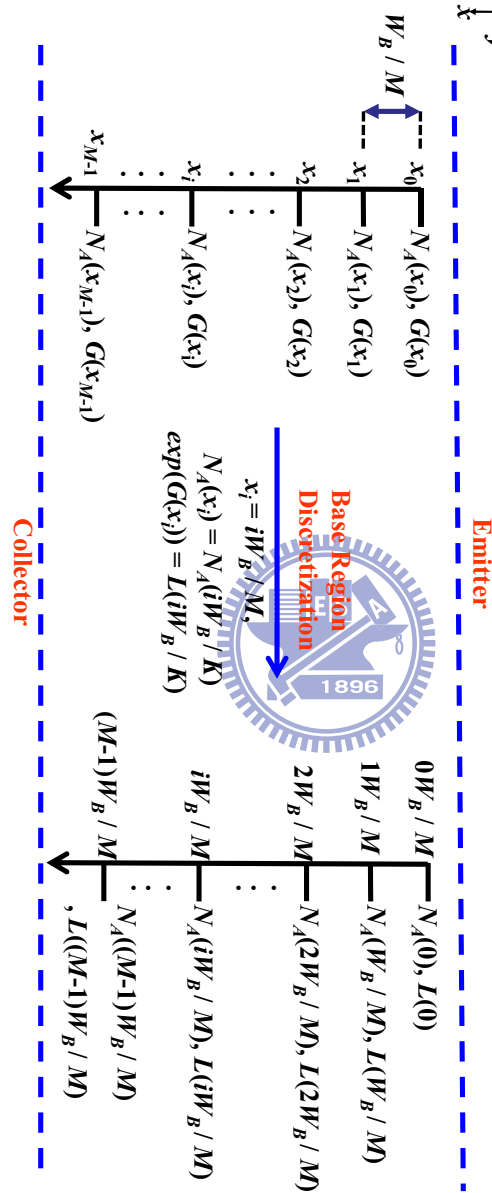
Figure 3.2: The discretization and variables transformation of integral (3.15). The base region in (3.15) is first discretized to M regions, $x_i = iW_B/M$, $i = 0, 1, ..., M-1$, and the continuous doping profile functions $N_A(x)$ and $G(x)$ can be transformed to $N_A(x_i)$ and $G(x_i)$, $i = 0, 1, ..., M-1$. Second we assume $L(x_i) = \exp(G(x_i))$, $i = 0, 1, ..., M-1$, and then the discretized doing profile function could be obtained.

and then problem (3.26) is reformulated as:

$$
\text{Min} \quad \log \left(\begin{array}{l} A \exp(\pi_0) + B_1 \exp(\alpha_0)^{0.5} \exp(\lambda_0)(1 + K_{SiGe}Ge_{AVG})^{-1} \\[2mm] + B_2 \exp(\lambda_0)(1 + K_{SiGe}Ge_{AVG})^{-1} + C \end{array} \right)
$$

$$
\begin{aligned}
s.t. \quad & N_{min} \le \log\left[\exp(\alpha_i)\right] \le N_{max}, \ i = 0, 1, ..., M-1 \\[2mm]
& \log\left[\exp(\eta_{i+1}) + \exp(\beta_i)^{-u}\exp(\alpha_i)^{1+\gamma_1-\gamma_2}\right] \le \log\left[\exp(\eta_i)\right], i = 0, 1, ..., M-1 \\[2mm]
& \log\left[\exp(\pi_{i+1}) + \exp(\beta_i)^{u}\exp(\alpha_i)^{\gamma_2-1}\exp(\eta_i)\right] \le \log\left[\exp(\pi_i)\right], i = 0, 1, ..., M-1 \\[2mm]
& \log\left[\exp(\lambda_{i+1}) + \exp(\alpha_i)^{1+\gamma_1-\gamma_2}\right] \le \log\left[\exp(\lambda_i)\right], i = 0, 1, ..., M-1 \\[2mm]
& \log\left[\exp(\pi_{M-1})^{-u}\exp(\alpha_{M-1})^{1+\gamma_1-\gamma_2}\right] = \log\left[\exp(\eta_{M-1})\right] \\[2mm]
& \log\left[\exp(\pi_{M-1})^{u}\exp(\alpha_{M-1})^{\gamma_2-1}\exp(\eta_{M-1})\right] = \log\left[\exp(\pi_{M-1})\right] \\[2mm]
& \log\left[\exp(\alpha_{M-1})^{1+\gamma_1-\gamma_2}\right] = \log\left[\exp(\lambda_{M-1})\right] \\[2mm]
& 1 \le \log\left[\exp(\beta_i)\right] \le \exp(G_{\max}) \\[2mm]
& \log\left[\exp(\alpha_i)\right] = \log\left[\exp(bx^m)\right], \ i = 0, 1, ..., 0.05M \\[2mm]
& \log\left[\exp(MGe_{AVG})\right] = \log\left[\prod_{i=0}^{M-1}\exp(\beta_i)\right]
\end{aligned}
$$

$$(3.28)$$

Eq. (3.28) is a convex programming since the objective is a convex function, and all the inequalities are convex inequality constraints since the left-hand sides of the inequalities are exponential functions and the respect right-hand sides are affine functions; and the equalities constraints are all affine functions. For the convex programming, based on the theorem 21.9 in [90], we could estimate the solution property of the modelled problem. As

shown below, we state the theorem:

Theorem: *Consider the general constrained optimization problem*

$$\text{Min} \quad f(x)$$

$$s.t. \quad h(x) = 0 \quad ,$$

$$g(x) \leq 0$$

if $f_0 : \Re^n \to \Re, f \in C^1$, *be a convex function on the set of feasible points*

$$\Omega = \{x \in \Re^n : h(x) = 0, g(x) \leq 0\}$$

where $h : \Re^n \to \Re^m, g : \Re^n \to \Re^p, h, g \in C^1$, *and* Ω *is a convex set, and if this problem is feasible, then the solution x* is a global minimizer of f over* Ω.

Now, according to the theorem, if the problem (3.28) has the solution, then we could guarantee the solution of the problem (3.28) and the original GP problem of (3.26) is global optimal.

3.3 Solving the SiGe HBTs Doping Profile Optimization Problem

We discretize problem (3.26) of total variables equal to 100, and solve this problem using the package ggplab [64]. The implemented codes are listed below:

Table 3.2: The adopted parameters for the forward and base transit time model. The W_{BC} is the base–collector depletion width, v_{sat} is the saturation velocity of electrons, W_E is the width of the emitter region, $P_{Eq,E}$ is the equilibrium concentration of holes in the emitter, γ is the ratio of the effective density of states in SiGe to the effective density of states in silicon. The k_{SiGe}, γ_2 and D_{n0} are constants.

Symbol	Value
W_{BC}	20 nм
V_{sat}	5×10^6 cm / s
W_E	300 nм
$P_{Eq,E}$	1.5×10^{10} cm^{-3}
K_{SiGe}	3
γ	0.87
D_{no}	20.72 cm^2/ s
γ_2	0.69

%—————Start program—————

clear all;

%—————Parameter setting—————

M = 100;%discretized numbers

WB = 10^(-5);%base region

Gmax = 0.25;%maximin value of Ge-content

CJBC = 0.8*10^(-13);%base-collector junction capacitance

RC = 0.4; %collector resistance

Q = 1.6*10^(-19); %electrical charge

ABE = 0.25; %area of the base-emitter junction

T = 300; %temperature (Kelvin)

ni0 = 1.4*(10^10); %intrinsic carrier concentration in a undoped Si

Nmax = 1*10^19; %the maximum doping concentration Nmin = 5*10^16;

VBE = 1; %the applied voltage across the emitter-base junction

Vbi = 1.1; %built-in potential voltage

WBC = 20*10^(-7); %base-collector width

Vsat = 8*10^(6); %saturation velocity of electrons

WE = 20*10^(-5); %width of the emitter region

PEQE = 5*10^(5); %equilibrium concentration of holes in the emitter

KsiGE = 3; %constants

Gama = 0.87; %constants

K = 8.617*10^(-5); %Boltzmann constant

g1 = 0.42; %constants

g2 = 0.69; %constants

Nref = 10^17; %constants

Dn0 = 20.72; %constants

KSiGe = 3; %constants
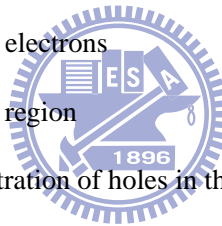
```
eSiGe = 1.04*10^(-12); %the permittivity of Si

u = 26.614; %constants

Gav = 0.09; a%verage ge fraction

b = 1; %constants

pwi = g2 -1; %constants

pwj = 1+g1-g2; %constants

%—————————End parameter setting—————————

% Define optimization

gpvar v(M) y(M) w(M) z(M) x(M) b(M)

% Background doping constraints

variables constr = [ Nmin*ones(M,1) <= v; v <=Nmax*ones(M,1);z<=exp(Gmax)*ones(M,1);];

% Recursive constraints for summation in objection function

for i=1:M-1

constr(end+1) = y(i+1) + (z(i)^(-u))*v(i)^pwj <= y(i);

constr(end+1) = (1/z(i))<=1;

constr(end+1) = w(i+1) + (z(i)^u)*y(i)*v(i)^pwi <= w(i);

constr(end+1) =x(i)==z(i)*x(i+1);

constr(end+1) = b(i+1) + v(i)^pwj <= b(i);

end
```

% The boundary of recursive constraints

constr(end+1) = y(M) == (z(M)^(-u))*(v(M)^pwj);

constr(end+1) = w(M) == (z(M)^u)*(y(M)*v(M)^pwi);

constr(end+1) = x(M) ==z (M) ;

constr(end+1) = b(M) == v(M)^pwj;

Assume 5% same doping profile

for i= 1:0.01*M

constr(end+1)=v(i)==v(i+1);

end

% Current gain constraint

last_constr_index = length(constr) + 1;

add=length(last_constr_index) + 1;

constr(last_constr_index) =x(1)==exp(M*Gav);

% Cut-off frequency model optimization

GBco= WB/(M*Nref^(g1-g2)*Dn0);

A = WB/(M^2*Nref^g1*Dn0)*(1+KSiGe*Gav));

B1 = (WE*PEQE/(2*ni0^2))*GBco*(gama^(-1)/(1+KSiGe*Gav))+

CJBC*K*T/(q^0.5*ABE*ni0^2)*exp(-q*VBE/(K*T))*

(gama^(-1)/(1+KSiGe*Gav))*GBco;

B2 = (K*T*(eSiGe*q^1.5/(ni0^2*2*(vbi-VBE)))^(0.5))*

exp(-q*VBE/(K*T))*(gama^(-1)/(1+KSiGe*Gav))*GBco;

C = WBC/(2*Vsat)+RC*CJBC;

obj = A*w(1)+B1*b(1)+B2*b(1)*v(1)^0.5+C;

% Solve the problem

optval sol status = gpsolve(obj, constr);

assign(sol)

% Ge-dose

% fprintf(1,'\n%2.22f\', log(z));

% Plot the optimal doping profile

nbw = 0:1/M:1-1/M;

semilogy(nbw,v,'LineWidth',2);

axis([0 1 1e16 1e18]);

xlabel('base');

ylabel('doping');

%—————End program—————

After implementing this code, the package ggplab will first transform the command (constraints and objective) into the matrix form based on its defined parser. After that, the

convex programming transformation for the GP problem will be activated and the interior-point method based algorithm will solve the prime and dual problem of the GP in convex form. Then the doping profile of Si and Ge will be globally extracted.

Chapter 4

Results and Discussion

In the first section, the limitation of doping concentration and model calibration are first discussed. Then the dependence of cut-off frequency and gain on Ge-dose and base doping profile are investigated. Due to the strong influence of the shape and content of Ge on the base transit time, the cut-off frequency and gain of SiGe HBTs are co-optimized which are subject to the aforementioned constraints.

4.1 Mesh Discretization and Solution Time

In problem (3.26), We first discretize the base region with $M = 100$, which have 500 total optimal variables, 400 linear constraints and 301 nonlinear constraints in our following studies. The corresponding CPU time is within 30 seconds in a personal computer with 2.8

GHz CPU and 2G RAM.

4.2   Limitation of Doping Concentration and Model Calibration

For the original GP model in Eq. (3.26), there is no constraint to restrict the doping profile. However, the stepwise doping profile is difficult to achieve in the realistic manufacturing process. A constraint of doping profile is then considered [36].

$$\left| N_A^{'}(x) \right| \leq \alpha N_A(x), \tag{4.1}$$

where α specifies the maximum allowed gradient and is adjustable to approximate the realistic doping profile. Figure 4.1 shows the doping profile of our device (0% Ge_{AVG}) with and without gradient constraint. The cut-off frequency of device with doping profile constraint is significantly smaller than that without constraint. The incorporation of gradient constraint of doping profile is crucial for realistic device doping profile optimization. To ensure the accuracy of the optimized doping profile, the doping profile is implemented in our in-house device simulator, as shown in Fig. 4.2 [84-88]. In device simulation, we first solved the time-dependent drift-diffusion equations with calibrated mobility models and generation-recombination models. After we obtained the DC operation point of device, the AC simulation is the applied to obtain the AC characteristics of HBT. In Fig. 4.2, the solid

line shows the optimized doping profile and the dashed line shows the doping profile realized in the two-dimensional device simulation. The cut-off frequency is then extracted by the 2D device simulation. The cut-off frequency in the two-dimensional device simulation approaches 70 GHz, which is very similar to the cut-off frequency in the GP model, 71 GHz. The result confirms the accuracy of the established GP model.
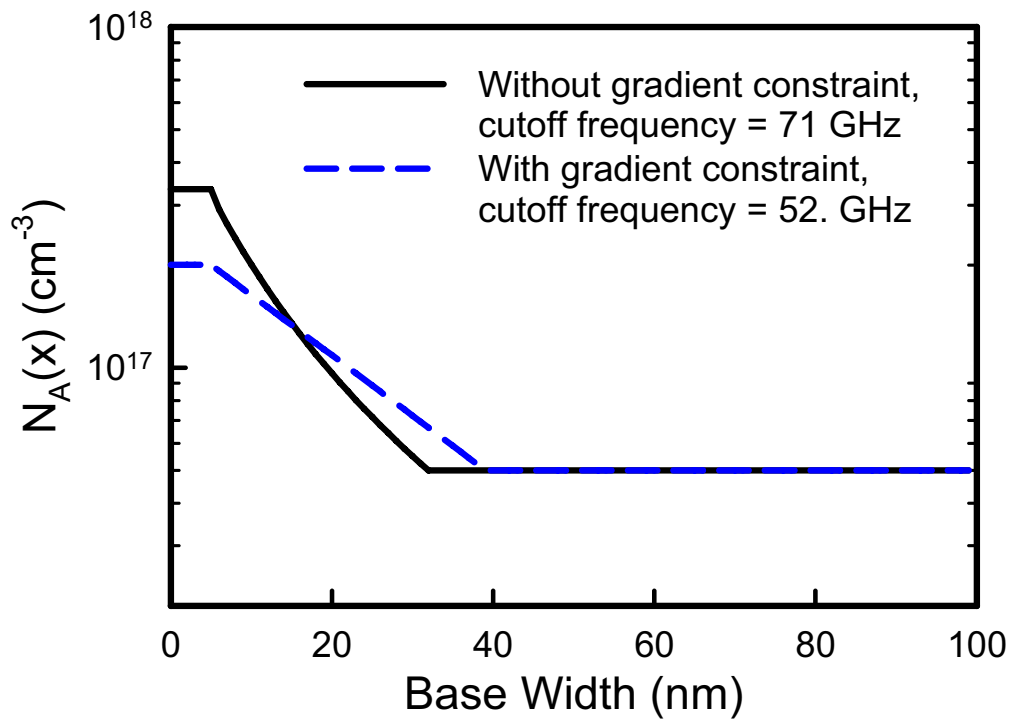
Figure 4.1: Optimized doping profile with and without gradient
constraint of doping profile, where the Ge-dose
concentration is set to be zero. The cut-off frequency of
device with doping profile constraint is significantly smaller
than that without constraint.

Figure 4.2: The doping profile obtained from GP model and the 2D
                device simulation. The doping profile of TCAD simulation
                is obtained by three different ion implantation processes.
                The cut-off frequency in the two-dimensional device
                simulation approaches 70 GHz, which is very similar to the
                cut-off frequency in the GP model, 71 GHz.
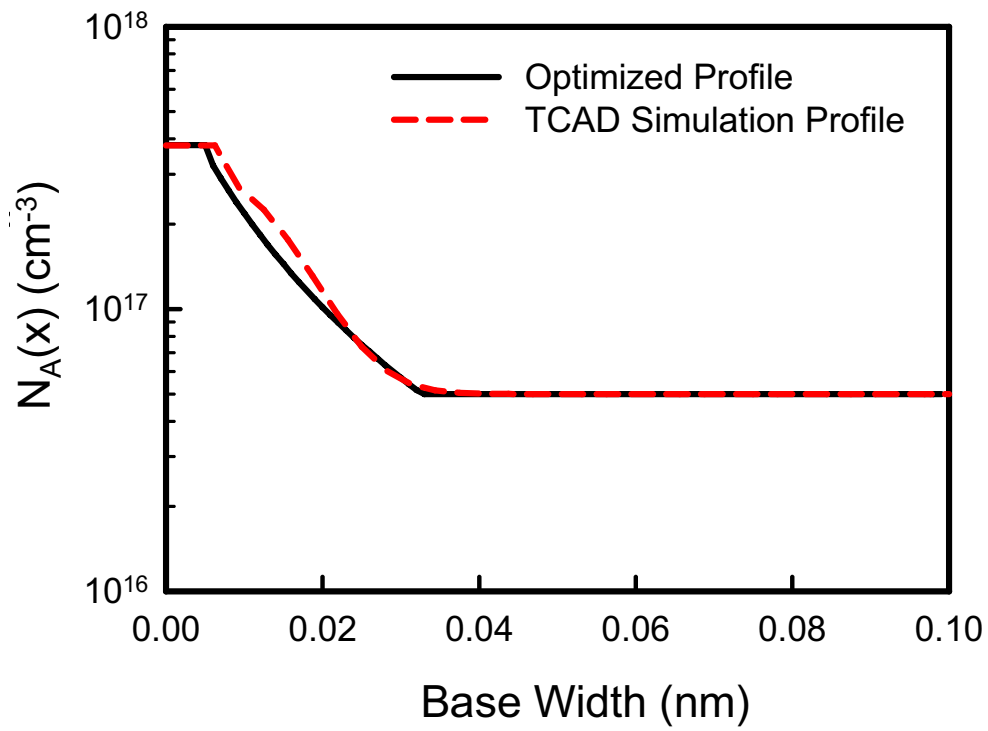
4.3   Cut-off Frequency Optimization

Figure 4.3 shows the SiGe HBT with various Ge-dose concentrations, 2%, 8% and 12.5%, respectively. The device with a higher Ge-dose concentration can exhibit a higher cut-off frequency. The obtained optimized doping profiles are changed with respect to different Ge-dose concentrations. The result shows a promising characteristic of SiGe HBT than a pure silicon device. The Ge profiles for HBTs with various Ge-dose concentrations, 2%, 8% and 12.5% are plotted in Fig. 4.4. Figure 4.5 presents the dependence of cut-off frequency as a function of Ge-dose concentration is then investigated. The addition of Ge-dose in silicon can provide a high cut-off frequency; however, the cut-off frequency is decreased as the Ge-dose is increased and higher than 12.5%. Besides, for the Ge-dose and base doping profile optimization, the background doping is also an important factor in device characteristic optimization. Figure 4.6 shows the impact of background doping profile on the cut-off frequency. As the background doping, N_{min}, is decreased from 5×10^{16} cm^{-3} to 3×10^{16} cm^{-3}, the obtained optimal cut-off frequency could be increased from 71 GHz to 85 GHz. Figure 4.7 plots Ge profile for devices with different background doping concentration. The Ge doping profiles are the same due to the same Ge_{Avg}. Figure 4.8 shows the cut-off frequency as a function of background doping profile and Ge-dose concentration. Since the cut-off frequency is increased as the Ge-dose concentration is decreased and the device with a maximum cut-off frequency is with 12.5% Ge-dose concentration.
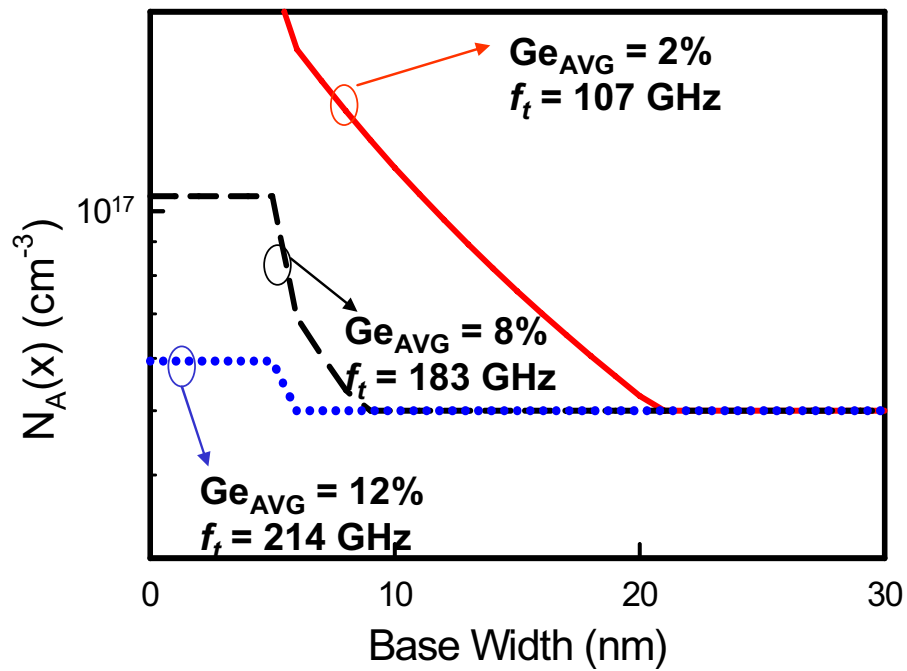
Figure 4.3: Doping profile and the corresponding cut-off frequency with 2%, 8%, and 12.5% Ge-dose concentration. The obtained optimized doping profiles and cut-off frequency are changed with respect to different Ge-dose concentrations.
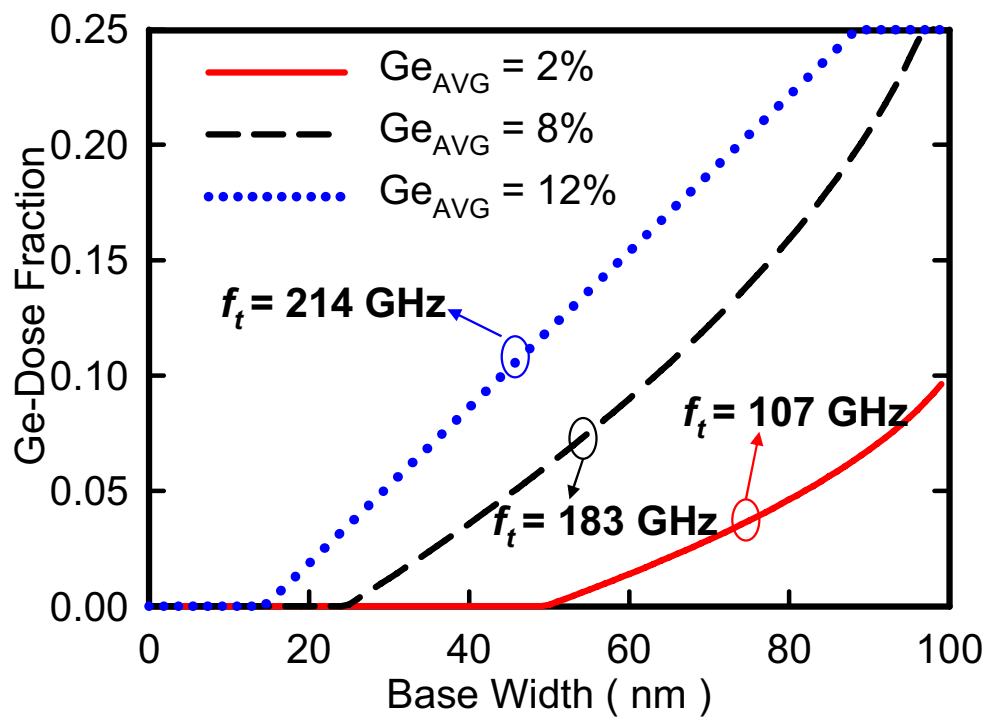
Figure 4.4: The Ge profiles for HBTs with 2%, 8%, and 12.5% Ge-dose
concentration. The cut-off frequency increases when the Ge
fraction raise.
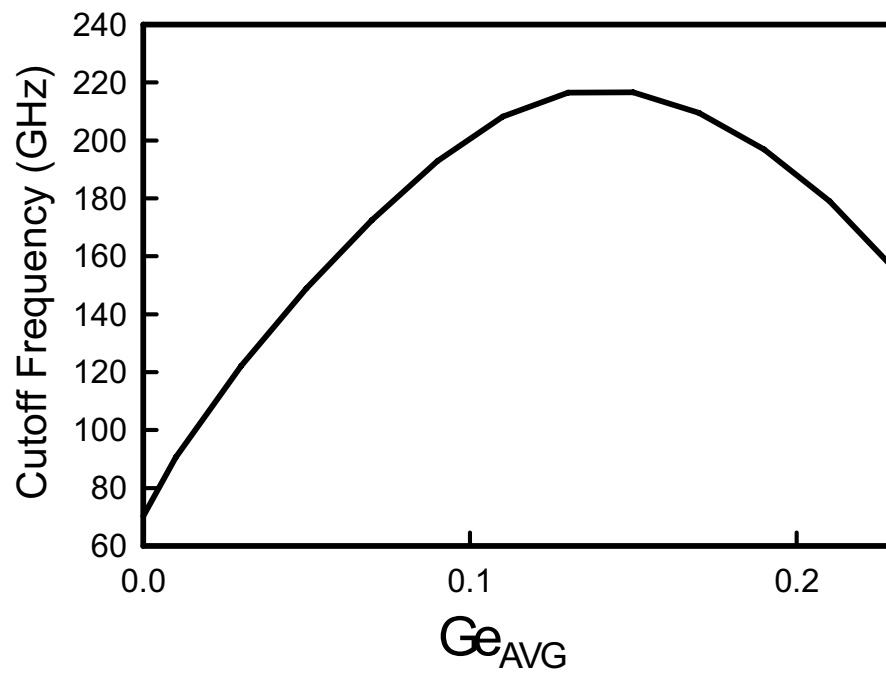
Figure 4.5: Cut-off frequency with various Ge-dose concentrations. The addition of Ge-dose in silicon can provide a high cut-off frequency; however, the cut-off frequency is decreased as the Ge-dose is increased and higher than 12.5%
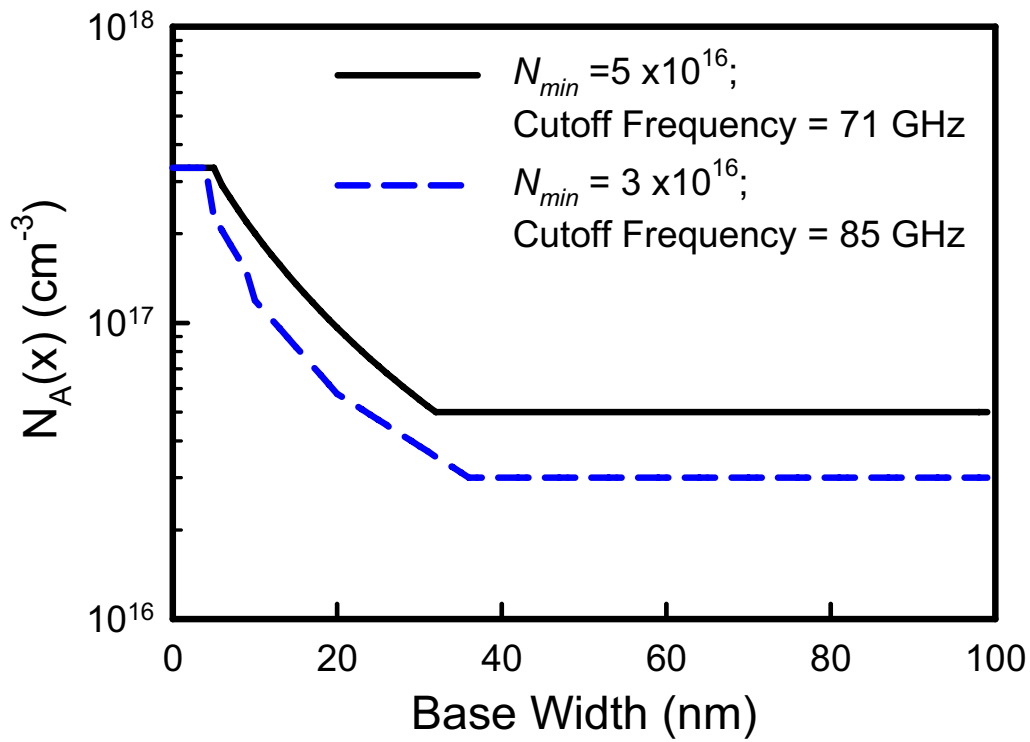
Figure 4.6: Doping profile of decreasing background doping to 3×10^{16} cm^{-3} for 3% Ge content. As the background doping, N_{min}, is decreased from 5×10^{16} cm^{-3} to 3×10^{16} cm^{-3}, the obtained optimal cut-off frequency could be increased from 71 GHz to 85 GHz.
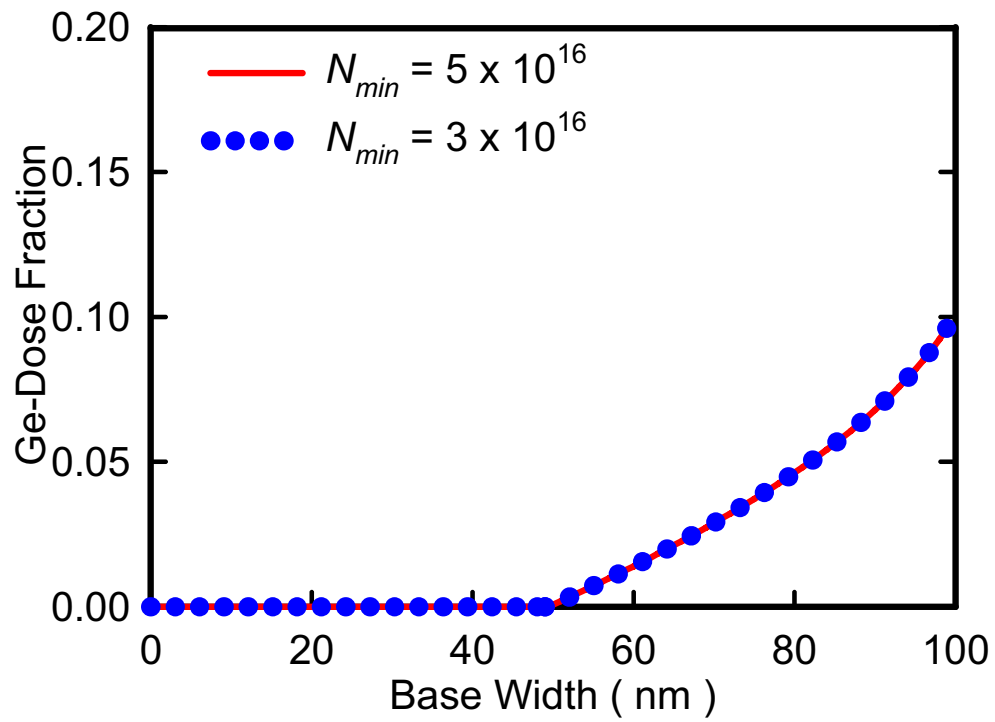
Figure 4.7: Doping profile of Ge for different background doping concentration of Si. The Ge doping profiles are the same due to the same Ge_{Avg} and is independent to background doping concentration.
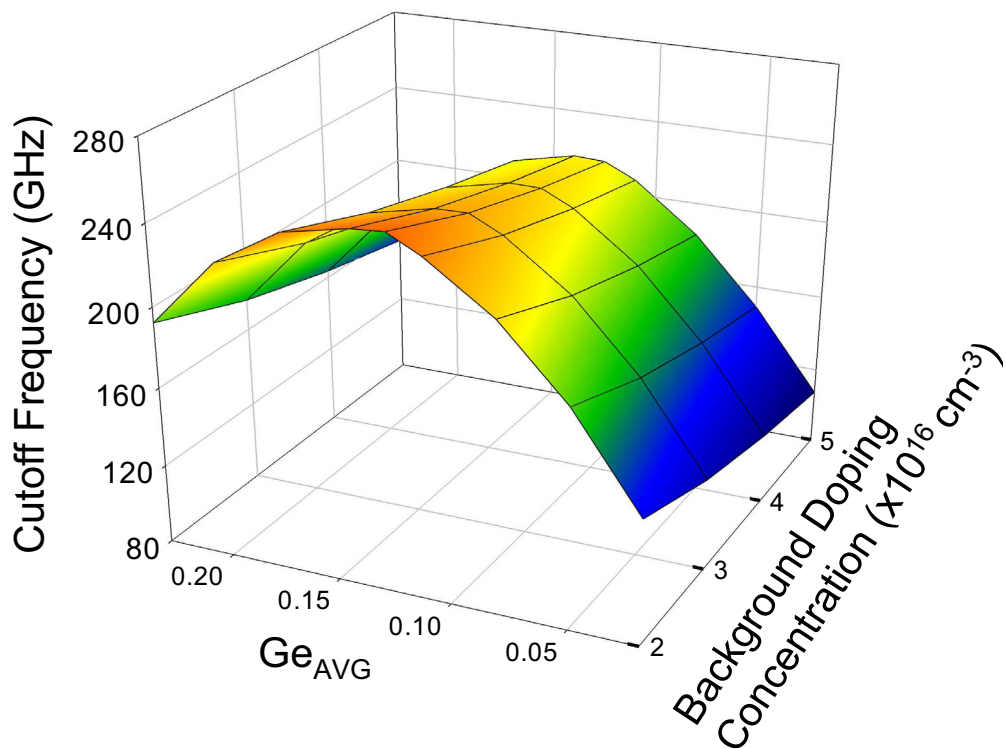
Figure 4.8: The cut-off frequency as a function of Ge-dose and
             background doping concentrations. The results exhibit the
             cut-off frequency is increased as the Ge-dose concentration
             reached 12.5 % while implanting lower background doping
             concentration.

4.4 Current Gain and Cut-off Frequency Co-Optimization

In addition, the optimization of cut-off frequency, the current gain, β of HBTs is crucial for communication application, which can be significantly influenced by the base doping profile. How to compromise the cut-off frequency and current gain of HBTs becomes a critical issue in SiGe technology. The current gain is defined by the ratio of collector and can be expressed as the ratio of Gummel numbers:

$$\beta = \frac{G_{E,SiGe}}{G_{B,SiGe}}, \tag{4.2}$$

where $G_{E,SiGe}$ is the emitter Gummel number and $G_{B,SiGe}$ is the base Gummel number. Since the emitter Gummel number depends mostly on the emitter doping profile, and thus can be treated as a positive constant in the optimization flow. For the base Gummel number, the dependence of Gummel number depends on the base doping profile has been studied in Eq. (3.8). Therefore, the relationship and Eq. (4.2) are then transformed as the current gain constraint and plugged to the GP model. Figure 4.9 shows the cut-off frequency as a function of the current gain. Since the cut-off frequency is related to the current gain and bandwidth, the obtained cut-off frequency will be smaller with a higher current gain constraint. The relation between cut-off frequency and current gain varies with different Ge-dose concentration. The device with 14% Ge-dose concentration exhibits the highest cut-off frequency. However, to obtain the maximum current gain, the device with the highest Ge-dose concentration exhibits a favorable characteristic. Moreover, the results show

that the device with a higher Ge-dose concentration could provide a higher gain and thus releases the design constraint. For each of the Ge content, the cut-off frequency is decreased with the increasing current gain constraint and then dropped significantly. The tuning point, in which the current gain constraint starts to significantly reduce the cut-off frequency, is decisive in obtaining the maximum current gain with sufficient cut-off frequency. Therefore, by careful selection of the maximum current gain constraint, we could find the optimal current gain constraint, $\beta/G_{E,SiGe} \times 10^{11}$, with sufficient cut-off frequency, as shown in Fig. 4.10, where the lower background doping concentration and higher Ge-dose concentration may provide the largest current gain.
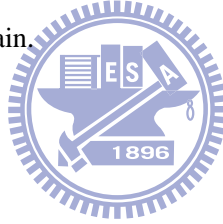
As shown in Fig. 4.8, it is found that 12.5% Ge-dose concentration and 2×10^{16} cm^{-3} background doping concentration can maximize the cut-off frequency. The higheset cut-off frequency can reach 254 GHz. On the other hand, for obtaining the maximum current gain, as shown in Fig. 4.10, the Ge-dose concentration is about 23% and the background doping is about 2×10^{16} cm^{-3}, where the maximized current gain constraint $\beta/G_{E,SiGe} \times 10^{11} =$ 1100, and the value of current gain β is about 1200. The obtained optimal doping profile and Ge-dose concentration are plotted in Fig. 4.11. Result shows that for the SiGe HBTs, the triangular Ge profiles are the best suited to achieve the minimum base transit time and trapezoidal Ge profiles are the best suited to get high current gain in SiGe HBTs,

which matches the practical design consideration of SiGe HBTs [35]. The design of Ge-dose concentration for obtaining high cut-off frequency and high current gain is rather different. Therefore, to compromise the purpose of high cut-off frequency, we use the cut-off frequency multiplies the current gain constraint as a new object function. The optimized result is shown in Fig. 4.12, similar to the result of current gain, shown in Fig. 4.10, the device with a higher Ge-dose concentration and a lower background doping concentration exhibits the best result. The optimal condition for maximum cut-off frequency-current gain product is at the point of Ge_{AVG} = 23% and N_{min} = 2 $\times$ 10^{16} cm^{-3}. The correspondent optimal doping profile and Ge profile are the dashed lines in Fig. 4.11. We notice that the object function, which is composed by the cut-off frequency and the current gain, could be adjusted according to designer's interest.
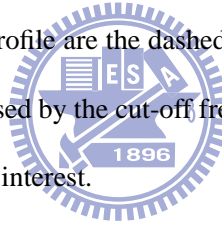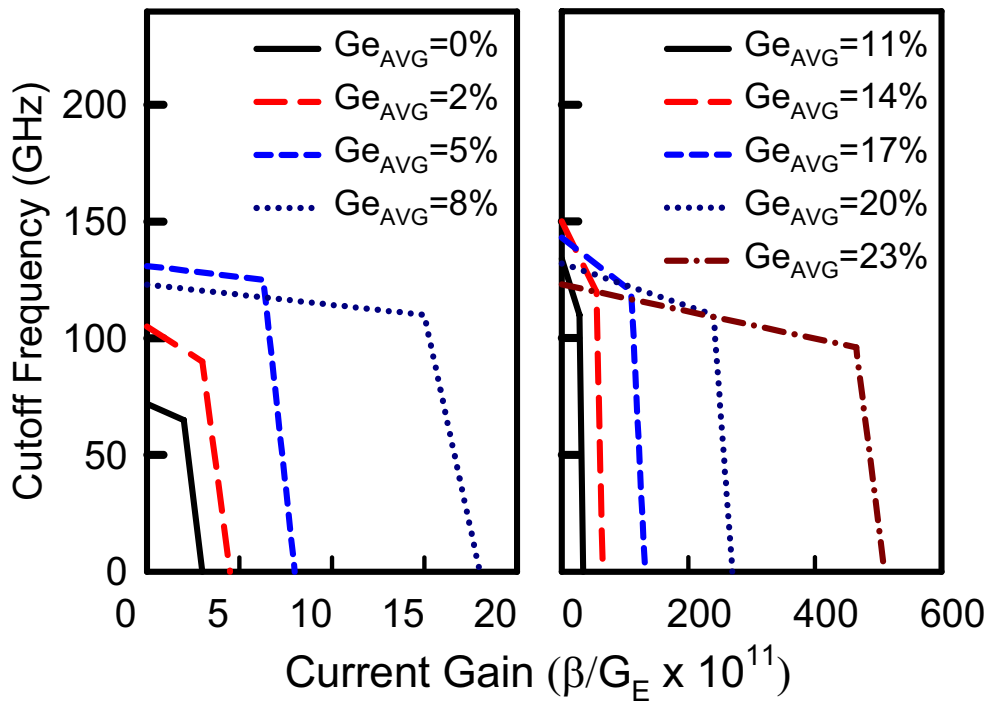
Figure 4.9: The maximized current gain constraint can add for 0% to
23% Ge content. The device with 14% Ge-dose
concentration exhibits the highest cut-off frequency.
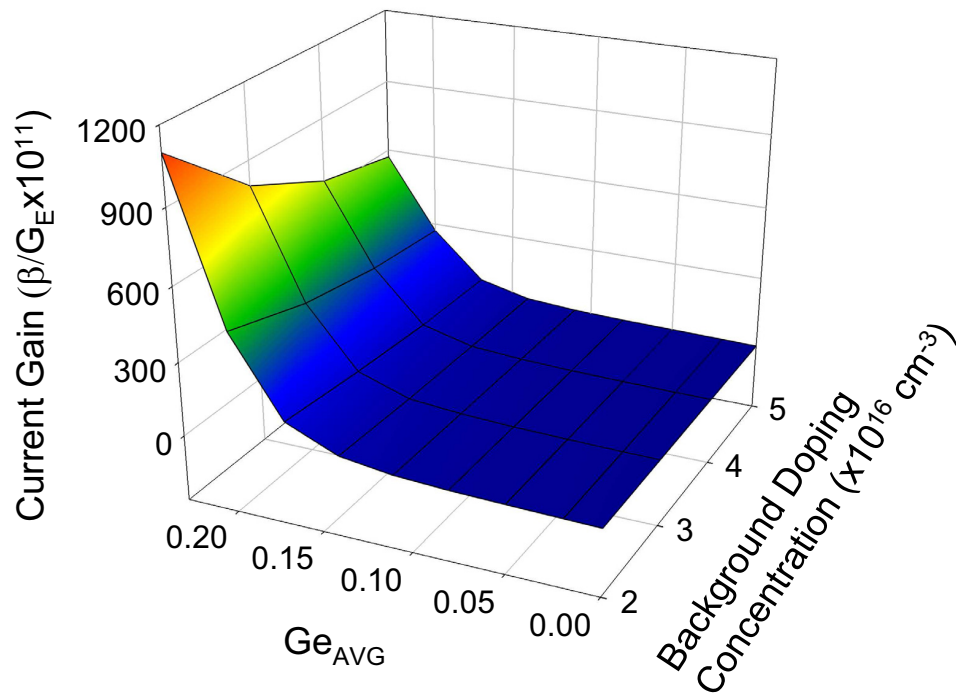
Figure 4.10: The maximum current gain constraint, which is added for every Ge content and background doping to maintain sufficient cut-off frequency. The lower background doping concentration and higher Ge-dose concentration may provide the largest current gain.
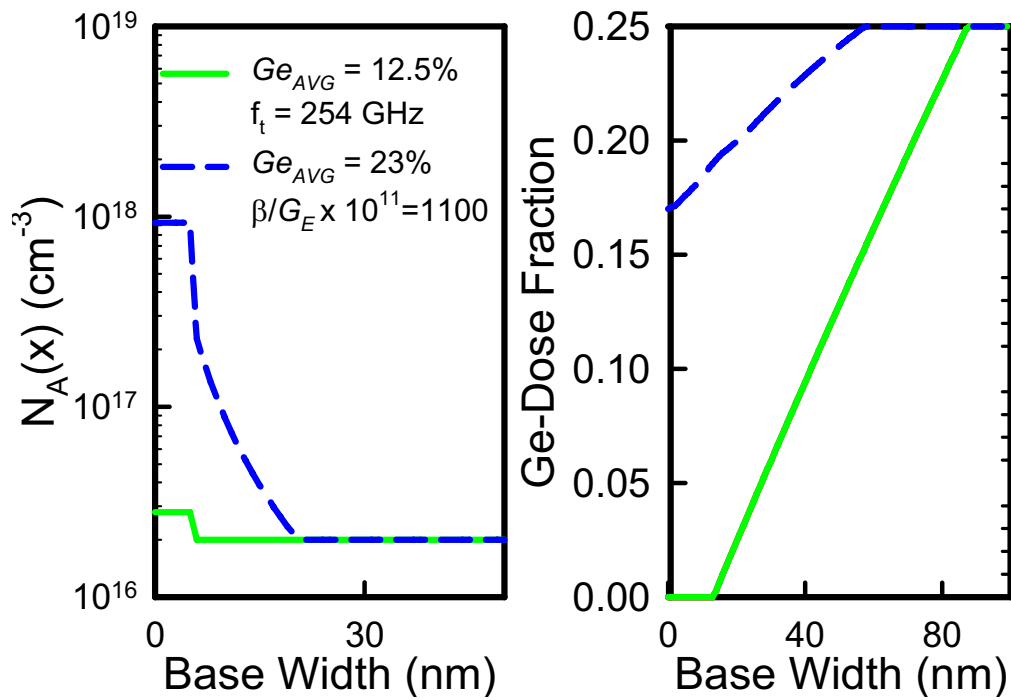
Figure 4.11:   Optimal Si and Ge doping profile for cut-off frequency
                maximize and maximize current gain constraint. The
                triangular Ge profiles are the best suited to achieve the
                minimum base transit time and trapezoidal Ge profiles are
                the best suited to get high current gain in SiGe HBTs
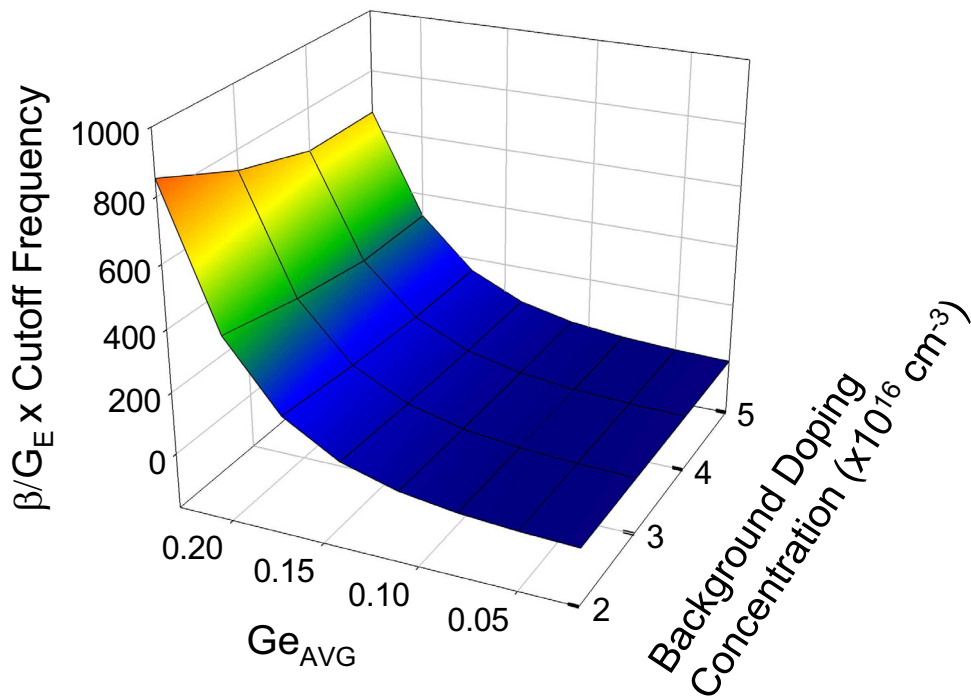
Figure 4.12: Co-optimization of cut-off frequency and current gain for
the SiGe HBTs. The trade-off surface shows that the
device with a higher Ge-dose concentration and lower
background doping concentration exhibits the best results.

Chapter 5

Conclusions

I n this chapter, we will draw the conclusion. In the section 5.1, we summarize this work. In the section 5.2, some future work are suggested.

5.1 Summary

In this study, the cut-off frequency and the current gain of SiGe HBT have been optimized via a geometric programming approach. The design of doping profile and the Ge concentration in the base region has been transformed into a convex optimization problem, and solved in a cost-effective manner. Our preliminary result has shown that a 23% Ge fraction may maximize the current gain; besides, a 12.5% Ge can maximize the cut-off frequency,

where 254 GHz cut-off frequency has been achieved. For the SiGe HBTs, the triangular Ge profiles are best suited to achieve the minimum base transit time and trapezoidal Ge profiles are best suited to get high current gain in SiGe HBTs. The accuracy of the adopted optimization technique was first confirmed by comparing with two-dimensional device simulation; consequently, the employed approach is computationally efficient and guarantees to always find the globally optimal solution. For concurrently optimization of multiple dopants in device channel, unlike other optimization approaches, which cycles through optimizing each one dopant species with the others fixed, this approach may give the optimal solution without the iteration. The GP formulation of device characteristics provides an alternative way to design of SiGe HBTs. The major contributions of this work are the transformation of cut-off frequency into a GP form for multiple doses doping profile optimization, additional and background doping of silicon substrate current gain consideration, and the validation of the analytic formula with by device simulation.

5.2 Future Work

1. The HBT devices could be fabricated based on the proposed optimal doping profile methodology.

2. The doping profile optimization of multi-finger HBT could also be investigated.

3. The method also handles other devices, such as MOSFETs, Fin-FET devices and static

random access memories.

4. For further precise calculation to sub-100 nm devices, the *posynomial* derivative of quantum effect correction model is necessary.

5. The proposed device doping profile optimization method could co-optimize with integrated circuits.

6. The commentary geometric programming [89] transformation for solving general nonlinear optimization could be further investigated.

7. Evolutionary algorithm combined geometric programming for solving general nonlinear programming could be developed.

8. For large scale GP problems, relaxed primal and dual path-following algorithms could be further implemented [91].
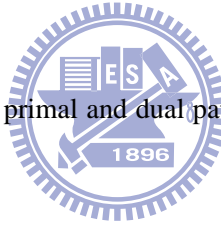
Bibliography

[1] J. W. Matthews and A. E. Blakeslee, "Defects in Epitaxial MultilayersX I: Misfit Dislocations in Layers," *Journal of Crystal Growth* , vol. 27, 1974, pp. 118-125.

[2] G. L. Patton, J. H. Comfort, B. S. Meyerson, E. F. Crabbe, G. J. Scilla, E. de Fresart, J. M. C. Stork, J. Y.-C. Sun, D. L. Harame, and J. Burghartz, "75 GHz ft SiGe Base Heterojunction Bipolar Transistors," *IEEE Electron Device Letters*, vol. 11, Apr. 1990, pp. 171-173.

[3] J. H. Comfort, G. L. Patton, J. D. Cressler, W. Lee, E. F. Crabbe, B. S. Meyerson, J. Y.-C. Sun, J. M. C. Stork, P.-F. Lu, J. N. Burghartz, J. Warnock, K. Kenkins, K.-Y. Toh, M. DAgostino, and G. Scilla, "Profile Leverage in A Self-Aligned Epitaxial Si or SiGe-Base Bipolar Technology," in *Technical Digest - International Electron Devices Meeting*, 1990, pp. 21-24.

[4] D. L. Harame, E. F. Crabbe, J. D. Cressler, J. H. Comfort, J. Y.- C. Sun, S. R. Stiffler,
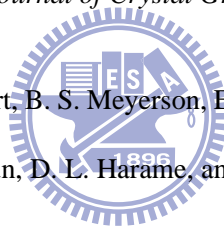
E. Kobeda, J. N. Burghartz, M. M. Gilbert, J. Malinowski, and A. J. Dally, "A High-Performance Epitaxial SiGe base ECL BiCMOS Technology," in *Technical Digest - International Electron Devices Meeting*, 1992, pp. 19-22.

[5] D. L. Harame, J. M. C. Stork, B. S. Meyerson, K. Y.-J. Hsu, J. Cotte, K. A. Jenkins, J. D. Cressler, P. Restle, E. F. Crabbe, S. Subbanna, T. E. Tice, B. W. Scharf, and J. A. Yasaitis, "Optimization of SiGe HBT Technology for High Speed Analog and Mixed-signal Applications," in *Technical Digest - International Electron Devices Meeting*, 1993, pp. 71-74.

[6] E. Kasper, A. Gruhle, and H. Kibbel, "High Speed SiGe-HBT with Very Low Base Sheet Resistivity" in *Technical Digest - International Electron Devices Meeting*, 1993, pp. 79-81.

[7] E. F. Crabbe, B. S. Meyerson, J. M. C. Stork, and D. L. Harame, "Vertical Profile Optimization of Very High Frequency Epitaxial Siand SiGe-base Bipolar Transistors," in *Technical Digest - International Electron Devices Meeting*, 1993, pp. 83-86.

[8] A. Schuppen, A. Gruhle, U. Erben, H. Kibbel, and U. Konig, "Multiemitter Finger SiGe HBTs with fmax up to 120 GHz," in *Technical Digest - International Electron Devices Meeting*, 1994, pp. 377-380.

[9] D. L. Harame, K. Schonenberg, M. Gilbert, D. Nguyen-Ngoc, J. Malinowski, S.-J. Jeng, B. S. Meyerson, J. D. Cressler, R. Groves, G. Berg, K. Tallman, K. Stein, G. Hueckel, C. Kermarrec, T. Tice, G. Fitzgibbons, K. Walter, D. Colavito, T. Houghton, N. Greco, T. Kebede, B. Cunningham, S. Subbanna, J. H. Comfort, and E. F. Crabbe, "A 200 mm SiGe-HBT Technology for Wireless and Mixedsignal Applications," in *Technical Digest - International Electron Devices Meeting*, 1994, pp. 437-440.

[10] J. N. Burghartz, J. H. Comfort, G. L. Patton, J. D. Cressler, B. S. Meyerson, J. M. C. Stork, J. Y.-C. Sun, G. Scilla, J. Warnock, K. Jenkins, K.-Y. Toh, D. L. Harame, and S. R. Mader, "Sub-30 ps ECL Circuits Using High ft Si and SiGe Epitaxial SEEW Transistors," in *Technical Digest - International Electron Devices Meeting*, 1990, pp. 297-300.

[11] E. F. Crabbe, J. H. Comfort, J. D. Cressler, J. Y.-C. Sun, and J. M. C. Stork, "High-Low Polysilicon-Emitter SiGe-Base Bipolar Transistors," *IEEE Electron Device Letters*, vol. 14, Oct. 1993, pp. 478-480.

[12] D. Harame, L. Larson, M. Case, K. Kovacic, S. Voinigescu, T. Tewksbury, D. Nguyen-Ngoc, K. Stein, J. D. Cressler, S.-J. Jeng, J. Malinowski, R. Groves, E. Eld, D. Sunderland, D. Rensch, M. Gilbert, K. Schonenberg, D. Ahlgren, S. Rosenbaum, J. Glenn, and B. Meyerson, "SiGe HBT Technology: Device and Application

Issues," in *Technical Digest - International Electron Devices Meeting*, 1995, pp. 731-734.

[13] F. Sato, T. Hashimoto, T. Tatsumi, M. Soda, H. Tezuka, T. Sazaki, and T. Tashiro, "A Self-Aligned SiGe Base Bipolar Technology Using Cold Wall UHV/CVD and its Application for Optical Communications ICs," in *Proceedings of IEEE Bipolar/BiCMOS Circuits Technollogy Meeting*, 1995, pp. 82-88.

[14] A. Pruijmboom, D. Terpstra, C. Timmering, W. deBoer, M. Theunissen, J. Slotboom, R. Hueting, and J. Hageraats, "Selective-Epitaxial Base Technology with 14 ps ECL-Gate Delay for Low Power Wide-Band Communications Systems," in *Technical Digest - International Electron Devices Meeting*, 1995, pp. 747-750.

[15] D. Ahlgren, M. Gilbert, D. Greenberg, S.-J. Jeng, J. Malinowski, D. Nguyen-Ngoc, K. Schonenberg, K. Stein, D. Sunderland, R. Groves, K. Walter, G. Hueckel, D. Colavito, G. Freeman, D. Harame, and B. Meyerson, "Manufacturability Demonstration of An Integrated SiGe HBT Technology for the Analog and Wireless Marketplace," in *Technical Digest - International Electron Devices Meeting*, 1996, pp. 859-862.

[16] M. Kondo, K. Oda, E. Ohue, H. Shimamoto, M. Tanabe, T. Onai, and K. Washio,

"Sub-10 fJ ECL/68 A 4.7 GHz Divider Ultra-Low-Power SiGe Base Bipolar Transistors with A Wedge-Shaped CVD-SiO2 Isolation Structure and a BPSG-Refilled Trench," in *Technical Digest - International Electron Devices Meeting*, 1996, pp. 245-248.

[17] D. Ahlgren, G. Freeman, S. Subbanna, R. Groves, D. Greenberg, J. Malinowski, D. Nguyen-Ngoc, S. Jeng, K. Stein, K. Schonenberg, D. Kiesling, B. Martin, S. Wu, D. Harame, and Meyerson, "A SiGe HBT BiCMOS Technology for Mixed-Aignal RF Applications," in *Proceedings of IEEE Bipolar/BiCMOS Circuits Technollogy Meeting*, 1997, pp. 195-197.

[18] E. de Berranger, S. Brodnar, A. Chantre, J. Kirtsch, A. Monroy, A. Granier, M. Laurens, J. L. Regolini, and M. Moulis, "Integration of SiGe Heterojunction Bipolar Transistors in a 200 mm Industrial BiCMOS Technology," *Thin Solid Films*, vol. 294, 1997, pp. 250-253.

[19] F. Sato, T. Hashimoto, T. Tatsumi, and T. Tashiro, "Sub-20 ps ECL circuits with High-Performance Super Self-Aligned Selectively Grown SiGe Base (SSSB) Bipolar Transistors," *IEEE Transactions on Electron Devices*, vol. 42, Mar. 1995, pp. 483-488.

[20] W. Gao, W. Snelgrove, T. Varelas, S. Kovacic, and D. Harame, "A 5-GHz SiGe

HBT Return-to-Zero Comparator," in *Proceedings of IEEE Bipolar/BiCMOS Circuits Technollogy Meeting*, 1995, pp. 166-169.

[21] H. Schumacher, U. Erben, A. Gruhle, H. Kibbel, and U. KLonig, "A 3 V Supply Voltage, DC-18 GHz SiGe HBT Wide-Band Amplifier," in *Proceedings of IEEE Bipolar/BiCMOS Circuits Technollogy Meeting*,1995, pp. 190-193.

[22] A. Gruhle, A. Scuppen, U. KLonig, U. Erben, and H. Schumacher, "Monolithic 26 GHz and 40 GHz VCOs with SiGe Heterojunction Bipolar Transistors, in *Technical Digest - International Electron Devices Meeting*, 1995, pp. 725-728.

[23] L. Larson, M. Case, S. Rosenbaum, D. Rensch, P. MacDonald, M. Matloubian, M. Chen, D. Harame, J. Malinowski, B. Meyerson, M. Gilbert, and S. Maas, "Si/SiGe HBT Technology for Low-Cost Monolithic Microwave Integrated Circuits," in *Technical Digest IEEE International Solid-State Circuits Conference*, 1996, pp. 80-81.

[24] F. Sato, H. Tezuka, M. Soda, T. Hashimoto, T. Suzaki, T. Tatsumi, T. Morikawa, and T. Tashiro, "A 2.4 Gb/s Receiver and A 1:16 Demultiplexer in One Chip Using A Super Self-Aligned Selectively Grown SiGe Base (SSSB) Bipolar Transistor," *IEEE Journal of Solid-State Circuits*, vol. 7, Oct. 1996, 1451-1457.

[25] R. GLotzfried, T. Itoh, J. F. Luy, and H. Schumacher, "Zero Power Consumption

Si/SiGe HBT SPDT T/R Antenna Switch," in *Technical Digest IEEE MTT-S International Microwave Symposium*, 1996, pp. 651-653.

[26] J. Long, M. Copeland, S. Kovacic, D. Malhi, and D. Harame, "RF Analog and Digital Circuits in SiGe Technology," in *Technical Digest IEEE International Solid-State Circuits Conference*, 1996, pp. 82-83.

[27] W. Gao, W. Snelgrove, and S. Kovacic, "A 5-GHz SiGe HBT Return-Tozero Comparator for RF A/D Conversion," *IEEE Journal of Solid-State Circuits*, vol. 31, 1996, pp. 1502-1506.

[28] M. Wurzer, T. Miester, H. Scafer, H. Knapp, J. BLock, R. Stengl, K. Aufinger, M. Franosch, M. Rest, M. MLoller, H. M. Rein, and A. Felder, "42 GHz Static Frequency Divider in Si/SiGe Bipolar Technology," in *Technical Digest IEEE International Solid-State Circuits Conference*, 1997, pp. 122-123.

[29] J. D. Cressler, "SiGe HBT Technology: A New Contender for Si-Based RF and Microwave Circuit Applications," *IEEE Transactions on Microwave Theory and Technical*, 1998, pp. 572-585.

[30] E. Ramirez-Garcia, N. Zerounian , P. Crozat, M. Enciso-Aguilar, P. Chevalier, A. Chantre, F. Aniel "SiGe Heterojunction Bipolar Transistor Issues Towards High Cryogenic Performances," *Cryogenics*, vol. 49, 2009, pp. 620-625.

[31] S. J. Jeng, B. Jagannathan, J.-S. Rieh, J. Johnson, K. T. Schonenberg, D. Greenberg, A. Stricker, H. Chen, M. Khater, D. Ahlgren, G. Freeman, K. Stein, and S. Subbanna "A 210-GHz fT SiGe HBT With a Non-Self-Aligned Structure," *IEEE Electron Device Letters*, vol. 22, 2001, pp. 542-544.

[32] D. L. Harame, J. H. Comfort, J. D. Cressler, E. F. Crabbe, J. Y.-C. Sun, B. S. Meyerson, and T. Tice, "Si/SiGe Epitaxial-Base Transistors: Part I-Materials, physics, and circuits," *IEEE Transactions on Electron Devices*, vol. 40, Mar. 1995, pp. 455-468.

[33] J. Rieh, D. Greenberg, A. Stricker, and G. Freeman, "Scaling of SiGe HBTs," in *Proceedings of IEEE*, vol. 93, no. 9, Sep. 2005, pp. 1522-1538.

[34] S.Weinreb, J. C. Bardin, and H. Mani, "Design of Cryogenic SiGe Lownoise Amplifiers," *IEEE Transactions on Microwave Theory and Technical*, vol. 55, no. 11, Nov. 2007, pp. 2306-2312.

[35] G. Khanduri, "Simultaneous Optimization of Doping Profile and Ge-dose in Base in SiGe HBTs," in *IEEE Southeast Conference*, 2007, pp. 579-583.

[36] S. Joshi, S. Boyd and R. Dutton, "Optimal Doping Profile via Geometric Programming," *IEEE Transactions on Electron Devices*, vol. 52, 2005, pp. 2660-2675.

[37] A. H. Marshak, "Optimum Doping Distribution for Minimum Base Transit Time," *IEEE Transactions on Electron Devices*, vol. 14, 1967, pp. 190-194.

[38] S. S. Winterton, S. Searles, C. J. Peters,N. G. Tarr and D. L. Pulfrey, "Distribution of Base Dopant for Transit Time Minimization in a Bipolar Transistor," *IEEE Transactions on Electron Devices*, vol. 43, 1996, pp. 170-172.

[39] M. J. Kumar and V. S. Patri, "On the Iterative Schemes to Obtain Optimum Base Profiles for Transit Time Minimization in A Bipolar Transistor," *IEEE Transactions on Electron Devices*, vol. 48, 2001, pp. 1222-1224.

[40] S. Szeto and R. Reif, "Reduction of f by Nonuniform Base Bandgap Narrowing," *IEEE Electron Device Letters*, vol. 10, 1989, pp. 341-343.

[41] P. V. Wijnen and R. D. Gardner R-D, "A New Approach to Optimizing the Base Profile for High-Speed Bipolar Transistors," *IEEE Electron Device Letters*, vol. 11, 1990, pp. 149-155.

[42] P. Rinaldi and H. Schattler, "Minimization of the Base Transit Time in Semiconductor Devices Using Optimal Control," in *International Conference Dynamical Systems Differential Equations*, 2002, pp. 1-10.

[43] H. Kroemer, "Two Integral Relations Pertaining to the Electron Transport through A Bipolar Transistor with A Nonuniform Energy Gap in the Base Region," *Solid-State Electronics*, vol. 28, 1985, pp. 1101-1103.

[44] D. L. Harame, J. H. Comfort, J. D. Cressler, E. F. Crabbe, J. Y. C. Sun, B. Meyerson and T. Tice, "Si/SiGe Epitaxial-Base Transistors: Part I. Materials, Physics, and Circuits," *IEEE Transactions on Electron Devices*, vol. 42, 1995, pp. 455-468.

[45] V. S. Patri and M. J. Kumar M-J, "Profile Design Considerations for Minimizing Base Transit Time in SiGe HBTs," *IEEE Transactions on Electron Devices*, vol. 45, 1998, pp. 1725-1731.

[46] K. Suzuki K, "Optimum Base Doping Profile for Minimum Base Transit Time," *IEEE Transactions on Electron Devices*, vol. 38, 1991, pp. 2128-2133.

[47] T. C. Lu and J. B. Kuo, "A Closed-Form Analytic Forward Transit Time Model Considering Specific Models for Bandgap-Narrowing Effects and Concentration-Dependent Diffusion Coefficients for BJT Devices Operating at 77 K," *IEEE Transactions on Electron Devices*, vol. 40, 1993, pp. 766-772.

[48] G. Khanduri and B. Panwar, "Study of Base Doping Profile Effects on SiGe Heterojunction Bipolar Transistors Performance for All Levels of Injection," *Semiconductor and Science Technology*, vol. 21, 2006, pp. 486-493.

[49] Y. Li and K. Y. Huang, "A Novel Numerical Approach to Heterojunction Bipolar Transistor Circuit Simulation," *Computer Physics Communications*, vol. 152, 2003, pp. 307-316.

[50] Y. Taur and T. Ning T, Fundamentals of Modern VLSI Devices, Cambridge, UK: Cambridge University Press,1998.

[51] P. Ashburn, SiGe Heterojunction Bipolar Transistors New York: Wiley, 2003.

[52] K. Kim, J. Heo, S Kim, D Mangalaraj and Y Junsin, "Optimum Ge Profile for the High Cut-Off Frequency and the DC Current Gain of an SiGe HBT for MMIC," *IEEE Transactions on Electron Devices*, vol.40, 2002, pp. 584-587.

[53] C. Zener, "A Mathematical Aid in Optimizing Engineering Design," in *Proceedings of National Academy of Science*, vol. 47, 1961, pp. 537-539.

[54] R. J. Duffin, "Dual Problems and Minimum Cost," *SIAM Journal on Applied Mathematics*, vol. 10, 1962, pp. 119-123.

[55] R. J. Duffin, E. L. Peterson, and C. Zener, Geometric Programming-Theory and Applications: Wiley; 1967.

[56] C. Zener, Engineering Designed by Geometric Programming. Wiley; 1971.

[57] C. S. Beightler and D. T. Phillips, Applied Geometric Programming. New York: Wiley; 1976.

[58] S. Boyd and L. Vandenberghe, Convex Optimization. Cambridge, U.K.: Cambridge Univ. Press, 2004.

[59] Y. Nesterov and A. Nemirovsky, "Interior-Point Polynomial Methods in Convex Programming," *SIAM*, vol. 13, 1994, pp. 65-69.

[60] K. O. Kortanek, X. Xu, and Y. Ye, "An Infeasible Interior-Point Algorithm for Solving Primal and Dual Geometric Progams," *Mathematical Programming*, vol. 76, 1996, pp. 155-181.

[61] B. A. Murtagh and M. A. Saunders, "Minos 5.4 user's guide," Systems Optimization Lab., Stanford Univ., Stanford, CA, Dec. 1983, Tech. Rept. SOL 83-20R.

[62] R. J. Vanderbei, Linear Programming: Foundations and Extensions. Norwell, MA: Academic, 1997.

[63] A. R. Conn, N. I. M. Gould, and PH. L. Toint, LANCELOT: A Fortran Package for Large-Scale Nonlinear Optimization (Release A). New York: Springer-Verlag, vol. 17, 1992.

[64] GGPLAB: A Simple Matlab Toolbox for Geometric Programming. [Online] http://www.stanford.edu/boyd/ggplab/.

[65] A. B. Templeman, "Structure Design for Minimum Cost Using the Method of Geometric Programming," in *Proceedings of the Institute of Civil Engineering*, vol. 46, 1970, pp. 459-470.

[66] J. J. Dinkel and G. A. Kochenberger, "A Cofferdam Designed Optimization," *Mathematical Programming*, vol. 6, 1974, pp. 114-117.

[67] Y. Smeers and D. Tyteca, "Geometric Programming Model for the Optimal Design of Wastewater Treatment Plants," *Operation Research*, vol. 32, no. b2, 1984, pp. 314-342.

[68] J. R. McNamara, "Optimization Model for Regional Water Quality Management," *Water Resource Research*, vol. 12, no. 2, 1976, pp. 125-134.

[69] M. J. Rijckert and X. M. Martems, "Analysis and Optimization of the Williamsotto Process by Geometric Programming," *AIChE Journal*, vol. 20, no. 4, 1974, pp. 742-750.

[70] M. Avriel and D. J. Wilde, "Optimal Condenser Designed by Geometric Programming," *I&EC Process Design and Development*, vol. 6, 1967, pp. 256-263.

[71] H. Adeli and O. Kamal, "Efficient Optimization of Space Trusses," *Computer and Structures*, vol. 24, no. 3, 1986, pp. 501-511.

[72] L. J. Mancini and R. J. Piziali, "Optimal Design of Helical Springs by Geometric Programming," *Engineering Optimization*, vol. 2, 1976, pp. 73-81.

[73] G. D. Bouchey and C. S. Beightler, and B. V. Koen, "Optimization of Nuclear Systems by Geometric Programming," *Nuclear Science and Engineering*, vol. 44, 1971, pp. 267-272.

[74] V. Balachandran and D. Gensch, "Solving the Marketing-Mix Problem Using Geometric Programming," *Management Science*, vol. 21, 1974, pp. 160-171.

[75] M. O. Abou-El-Ata and K. A. M. Kotb, "Muti-Item EOQ Inventory Model with Varying Holding Cost under Two Restrictions: A Geometric Programming Approach," *Production Planning and Control*, vol. 8, 1997, pp. 608-611.

[76] M. Hershenson, S. Boyd, and T. Lee, "Optimal Design of A CMOS Op-Amp via Geometric Programming," *IEEE Transactions on Computer-Aided Design of Integrated Circuits and Systems*, vol. 20, no. 1, 2001, pp. 1-21.

[77] J. Dawson, S. Boyd, M. Hershenson, and T. Lee, "Optimal Allocation of Local Feedback in Multistage Amplifiers via Geometric Programming," *IEEE Transactions on Circuits and Systems I, Fundamental Theory and Applications*, vol. 48, no. 1, 2001, pp. 1-11.

[78] J. Vanderhaegen and R. Brodersen, "Automated Design of Operational Transconductance Amplifiers Using Reversed Geometric Programming," in *Proceedings of IEEE/ACM Design Automation Conference*, San Diego, CA, Jun. 2004, pp. 133-138.

[79] S. Boyd, S.-J. Kim, D. Patil, and M. Horowitz, "Digital Circuits Sizing via Geometric Programming," *Operations Research*, vol. 53, no. 6, 2005, pp. 899-932.

[80] S. Mohan, M. Hershenson, S. Boyd, and T. Lee, "Simple Accurate Expressions for Planar Spiral Inductances," *IEEE Journal of Solid-State Circuits*, vol. 34, no. 10, 1999, pp. 1419-1424.

[81] M. Hershenson, A. Hajimiri, S. Mohan, S. Boyd, and T. Lee, "Design and Optimization of LC Oscillators," in *Proceedings of IEEE/ACM International Conference Computer-Aided Design*, 1999, pp. 65-69.

[82] Y. C. Chen and Y. Li, "Temperature-Aware Floorplanning via Geometric Programming," *Mathematical and Computer Modelling*, vol. 51, April 2010, pp. 927-934.

[83] Z. Michalewicz, Genetic Algorithms + Data Structures = Evolution Programs, New York, Springer, 1996.

[84] Y. Li and H. M. Lu, "An Investigation of Magnetic Effects on Energy Gap for Nanoscale InAs/GaAs Semiconductor Rings and Dots," *IEICE Transactions on Electronics*, vol. 86, 2003, pp. 466-473.

[85] Y. Li and S. M. Yu, "A Two-Dimensional Quantum Transport Simulation of Nanoscale Double-Gate MOSFETs Using Parallel Adaptive Technique," *IEICE Transactions on Information and Systems*, vol. 87, 2004, pp. 1751-1758.

[86] Y. Li, J. Y. Huang and B. S. Lee, "Effect of Single Grain Boundary Position on Surrounding-Gate Polysilicon Thin Film Transistors," *Semiconductor and Science Technology*, vol. 23, 2008, 015019.

[87] Y. Li, "Hybrid Intelligent Approach for Modeling and Optimization of Semiconductor Devices and Nanostructures," *Journal of Computational and Applied Mathematics*, vol. 45, 2009, pp. 41-51.

[88] Y. Li and C. H. Hwang, "DC Baseband and High-Frequency Characteristics of Silicon Nanowire Field Effect Transistor Circuit," *Semiconductor and Science Technology*, vol. 24, 2009, 045004.

[89] M. Avriel and A. C. Williams, "Complementary Geometric Programming," *SIAM*, vol. 19, no. 1, 1970, pp. 125-141.

[90] E. K. P. Chong and S. H. ZAK, An Introduction to Optimization, Cambridge, New York: Wiley, 2008.

[91] T. M. Hwang, C. H. Lin and W. W. Lin, "A relaxed primal-dual path-following algorithm for linear programming," *Annals of Operations Research*, vol. 62, 1996, pp. 173-196.
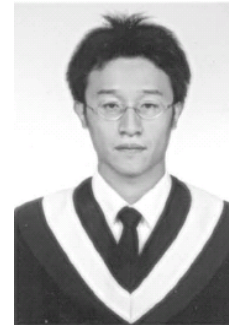
VITA

Name:Ying-Chieh Chen, 陳英傑

Permanent address: No. 274-3, Ln. 1, Anle St., Keelung City 204, Taiwan

Date of birth: February 7th, 1985

Place of birth: Keelung, Taiwan

Collegiate institutions attended	Degree	Date of graduate
Department of Transportation Technology and Management, National Chiao Tung University, Hsinchu, Taiwan	BS	June, 2008
Department of Electrical Engineering and Institute of Communication Engineering, National Chiao Tung University, Hsinchu, Taiwan	MS	August, 2010

Master thesis title: Doping Profile Optimization of silicon–germanium Heterojunction Bipolar Transistors via Geometric Programming

Publication List:

Journal papers
1. Yiming Li, **Ying-Chieh Chen** and Chih-Hong Hwang, "Doping Profile and Ge-Dose Optimization for Silicon-Germanium Heterojunction Bipolar Transistors," *Semiconductor Science and Technology*, vol. 24, no. 10, 105020, Sept. 2009.

2. **Ying-Chieh Chen** and Yiming Li, "Temperature Aware Floorplanning via Geometric Programming," *Mathematical and Computer Modeling*, vol. 51, pp. 927-934, April 2010.

Conference papers
1. Yiming Li and **Ying-Chieh Chen**, "High Frequency Property Optimization of Heterojunction Bipolar Transistor Using Geometric Programming," in *AIP Conference Proceedings*, 2007, vol. 963, pp. 997-1000.

2. Yiming Li and **<u>Ying-Chieh Chen</u>** and Chih-Hong Hwang, "Doping Profile and Ge-Dose Co-Design for Electrical Characteristic Optimization of SiGe HBT Devices," in *The IEEE International SiGe Technology and Device Meeting* (*IEEE ISTDM 2008*), Hsinchu, Taiwan, 2008.

3. Yiming Li, Chih-Hong Hwang and **<u>Ying-Chieh Chen</u>**, "High-Frequency Characteristic Optimization of Heterojunction Bipolar Transistors," in *Proceedings of the 2008 NSTI Nanotechnology Conference and Trade Show (NSTI Nanotech 2008), Boston, Massachusetts,* June 1-5, 2008, vol. 3, pp. 615-618.